

Federated Learning in the Presence of Adversarial Client Unavailability: Minimax Rates*

Lili Su

Electrical and Computer Engineering
Northeastern University

Ming Xiang

Electrical and Computer Engineering
Northeastern University

Jiaming Xu

The Fuqua School of Business
Duke University

Pengkun Yang

Center for Statistical Science
Tsinghua University

February 21, 2024

Abstract

Federated learning is a decentralized machine learning framework that enables collaborative model training without revealing raw data. Due to the diverse hardware and software limitations, a client may not always be available for the computation requests from the parameter server. An emerging line of research is devoted to tackling arbitrary client unavailability. However, existing work still imposes structural assumptions on the unavailability patterns, impeding their applicability in challenging scenarios wherein the unavailability patterns are beyond the control of the parameter server. Moreover, in harsh environments like battlefields, adversaries can selectively and adaptively silence specific clients. In this paper, we relax the structural assumptions and consider adversarial client unavailability. To quantify the degrees of client unavailability, we use the notion of ϵ -adversary dropout fraction. We show that simple variants of FedAvg or FedProx, albeit completely agnostic to ϵ , converge to an estimation error on the order of $\epsilon(G^2 + \sigma^2)$ for non-convex global objectives and $\epsilon(G^2 + \sigma^2)/\mu^2$ for μ -strongly convex global objectives, where G is a heterogeneity parameter and σ^2 is the noise level. Conversely, we prove that any algorithm has to suffer an estimation error of at least $\epsilon(G^2 + \sigma^2)/8$ and $\epsilon(G^2 + \sigma^2)/(8\mu^2)$ for non-convex global objectives and μ -strongly convex global objectives. Furthermore, the convergence speeds of the FedAvg or FedProx variants are $O(1/\sqrt{T})$ for non-convex objectives and $O(1/T)$ for strongly-convex objectives, both of which are the best possible for any first-order method that only has access to noisy gradients. Our proofs build upon a tight analysis of the selection bias that arises from adversarial client unavailability yet persists in the entire learning process.

1 Introduction

Federated learning is a decentralized machine learning framework wherein the parameter server and the clients collaboratively train machine learning models without having the clients disclose local data [1, 2]. Cross-device federated learning is often massive in scale and the availability of a client may be constrained by the diverse hardware and software limitations, making full client

*L. Su and M. Xiang are supported by the ARO Grant W911NF-23-2-0014. J. Xu is supported by the NSF Grants CCF-1856424 and CCF-2144593. P. Yang is supported by the NSFC Grant 12101353 and Tsinghua University Initiative Scientific Research Program.

participation impractical [1]. Most existing work either assumes that client unavailability follows benign distributions [1, 3, 4, 5] or that the parameter server can arbitrarily recruit participants [6], i.e., a client must adhere to the computation requests from the parameter server. There is a recent surge of interest in studying arbitrary client unavailability [7, 8, 9, 10]. Despite that they collectively laid a solid foundation in this direction, this line of work still imposes structural assumptions on unavailability patterns, impeding their applicability in challenging scenarios wherein the unavailability patterns are beyond the control of the parameter server. This is particularly relevant in non-controllable real-world environments wherein the availability of a client depends, in a complicated way, on multiple time-varying factors such as external interruptions and hardware/software status [1]. For instance, when the clients are mobile devices, a client may fail to respond to a computation request if disconnected from WiFi or if the communication connection is blocked by surrounding buildings or moving obstacles. A client may also suddenly abort federated learning due to factors such as low battery. Moreover, in harsh environments like battlefields, adversaries can selectively and adaptively silence specific clients.

In this paper, we relax those structural assumptions and consider adversarial client unavailability. Specifically, in each round, first the parameter server randomly samples K clients, and then a system adversary, based on all the information up to now, adaptively selects a subset of sampled clients to be non-responsive. To quantify the degrees of client unavailability, we use the notion of ϵ -adversary dropout fraction. It is worth noting that our adversarial client unavailability model can be viewed as a special case of Byzantine attacks [11, 12]. Nevertheless, existing Byzantine-resilient results do not apply to our problem. See Section 2 for details.

We show that simple variants of the standard FedAvg or FedProx algorithms, albeit agnostic to the degree of client unavailability ϵ , enjoy strong performance guarantees. We further validate our theories through numerical experiments on synthetic and real-world datasets. Specifically, we study a canonical setup in which the goal is to minimize $F(\theta) \triangleq \sum_{i=1}^M w_i F_i(\theta)$, where w_i is the weight and F_i is the local objective of client $i \in [M]$. The local data is non-IID yet satisfies the standard (B, G) -heterogeneity condition [2] (formally described in Assumption 3.1). Only noisy stochastic gradients are available. Our main theoretical results can be summarized in the following informal theorem.

Theorem 1.1 (Informal). *Let σ be the average noise level of the stochastic gradients. For $\sqrt{\epsilon}B \leq 0.1$,*

- *when F is non-convex:*

$$\frac{\epsilon(G^2 + \sigma^2)}{8} \leq \inf_{\hat{\theta}} \sup_{\mathcal{A}} \sup_{F_1, \dots, F_M} \mathbb{E}[\|\nabla F(\hat{\theta})\|^2] \leq 8\epsilon(G^2 + \sigma^2);$$

- *when F is μ -strongly convex:*

$$\frac{\epsilon(G^2 + \sigma^2)}{8\mu^2} \leq \inf_{\hat{\theta}} \sup_{\mathcal{A}} \sup_{F_1, \dots, F_M} \mathbb{E}[\|\hat{\theta} - \theta^*\|_2^2] \leq \frac{8\epsilon(G^2 + \sigma^2)}{\mu^2},$$

where \sup_{F_1, \dots, F_M} is taken over all local objectives that collectively satisfy the (B, G) -heterogeneity condition, \mathcal{A} is all adversarial client unavailability that is subject to ϵ -adversary dropout fraction, and $\inf_{\hat{\theta}}$ is taken over all algorithms $\hat{\theta}$ that have access to noisy local gradients only.

Importantly, the lower and upper bounds match each other up to a universal constant factor.

- The upper bounds are proved in Section 4 by analyzing variants of FedAvg or FedProx. We also characterize their convergence speeds to be $O(1/\sqrt{T})$ and $O(1/T)$, respectively. These convergence speeds are on par with the centralized settings [13, 14], and are the best possible for any first-order method that has only access to noisy gradients [15, 7].
- The threshold 0.1 of the assumption $\sqrt{\epsilon}B \leq 0.1$ is chosen for the ease of presentation. Our results continue to hold when $\sqrt{\epsilon}B \leq c_0$ as long as $c_0 < 1$ yet at the expense of inflating the estimation error upper bounds by a large constant factor. The assumption $\sqrt{\epsilon}B < 1$ is to some extent necessary. This is because as B increases, the F_i 's become more dissimilar, resulting in a reduced ability to tolerate adversarial dropouts.
- The lower bounds are shown in Section 6 (Theorem 6.1) for all algorithms (encompassing randomized and non-federated learning algorithms) and all $\epsilon \in (0, 1)$.

2 Related work

2.1 Partial client participation.

Most literature on partial client participation considers random client unavailability [2, 1, 3, 16, 4] with the implicit assumption that every selected client will respond to the computation requests from the parameter server. In parallel, the analysis on fastest responsive clients [3, 5, 2, 8] assumes that each client responds with a known probability.

A handful of work exists on arbitrary client unavailability [9, 7, 8, 10, 6]. Both [9] and [6] focus on controllable environments, where every client sampled by the parameter server must respond accordingly. Non-controllable environments were investigated more recently [7, 9, 8, 10] yet still imposes some structural requirements such as regularized participation [8], bounded inactive periods [9, 10, 7], and asymptotic unbounded inactive periods [7]. It is easy to find patterns that violate the aforementioned assumptions. For example, a client may be inactive for a while and become active at some carefully chosen time in order to disturb the learning process.

2.2 Byzantine-resilient distributed and federated learning.

Byzantine attack is a canonical adversary model in distributed computing [11]. In general, it includes two key components: (A.1) adversarial client selection, i.e., the compromised clients can be selected in the worst possible manner based on the knowledge of the system states, and (A.2) malicious value injection, i.e., the compromised clients inject arbitrary values into the system. Moreover, the subset of compromised client may vary over time [12, 11, 17], and can be adaptively chosen by the system adversary. Tolerating Byzantine attacks in distributed and federated learning have received intensive attention recently [18, 19, 20, 21, 22, 23, 24, 25, 26, 27, 28, 29]. Our adversarial unavailability model can be viewed as a special case of Byzantine attacks with adversarial client selection [i.e. (A.1)] but no malicious value injection [i.e., (A.2)]. Nevertheless, as we explain next, to the best of our knowledge, existing Byzantine-resilient results are not applicable to our problem. Both (A.1) and (A.2) that are adaptive to history information were considered in [22, 23, 30] yet under the simplified setting such as IID datasets, strongly-convex objectives, and one-step local updates. When the datasets are non-IID or unbalanced, unfortunately, the analysis therein breaks apart. Assuming the subset of Byzantine clients is pre-selected and fixed throughout training, a more recent line of work [28, 26, 27] focused on (A.2) only. IID local data is considered in [28, 26]. Extending their convergence analysis to non-IID settings is challenging unless imposing strong assumptions such as common stationary points or absolute bounded gradient dissimilarity.

It is crucial to assume the subset of Byzantine clients is pre-selected and fixed in [27, 29]. When the system adversary can adaptively choose different subsets of clients, the mean of each Byzantine-free bucket in [27] is no longer unbiased. To tolerate time-varying subsets of Byzantine clients, the (f, κ) -robustness in [29, Definition 2] requirement needs to be imposed on any client subset of proper size, which is hard to ensure unless the involved quantities follow light-tailed distributions such as subgaussian or subexponential [22, 23, 30].

3 System model

A parameter server and M clients collaboratively minimize

$$\min_{\theta \in \mathbb{R}^d} F(\theta) = \sum_{i=1}^M w_i F_i(\theta), \quad (1)$$

where $F_i(\theta) = \mathbb{E}_{z \sim \mathcal{D}_i} [\ell_i(\theta; z)]$ is the local objective, w_i is the weight, \mathcal{D}_i is the local data distribution, and $\ell_i(\theta; z)$ is a loss function. The local datasets can be unbalanced across clients. Let n_i denote the number of data points generated from the unknown \mathcal{D}_i at every round by client i , and $N = \sum_{i=1}^M n_i$ be the total number of data points drawn at every round. Following the literature [31, 3, 16, 32] we adopt the following bounded dissimilarity assumption.

Assumption 3.1 (Bounded dissimilarity). We say that (w_i, F_i) satisfies the (B, G) -bounded dissimilarity condition for $B \geq 1$ and $G \geq 0$ if $\sum_{i \in [M]} w_i \|\nabla F_i(\theta)\|_2^2 \leq B^2 \|\nabla F(\theta)\|_2^2 + G^2$.

When the local datasets are IID (i.e., $\mathcal{D}_i = \mathcal{D}_j$ for any $i, j \in [M]$), it holds that $B = 1$ and $G = 0$ as $F_i = F$ for all clients. When data is non-IID, more stringent forms of bounded dissimilarity assumptions are popular in the existing literature on arbitrary client unavailability and Byzantine resilience. For example, [9] and [6] assumed bounded gradients, i.e., $\sum_{i \in [M]} w_i \|\nabla F_i(\theta)\|_2^2 \leq G^2$. Both [8] and [10] assumed $\sum_{i \in [M]} w_i \|\nabla F_i(\theta) - \nabla F(\theta)\|_2^2 \leq G^2$. Byzantine resilience was shown in [27, 29] assuming either $G = 0$ or $\sum_{i \in [M]} w_i \|\nabla F_i(\theta) - \nabla F(\theta)\|_2^2 \leq G^2$.

Non-Static Client Unavailability. In each round t , first the parameter server uniformly at random selects a set $\tilde{\mathcal{S}}_t \subset [M]$ of K clients. Each client $i \in \tilde{\mathcal{S}}_t$ draws a fresh sample $z_{i,t}$ of size n_i from the local dataset \mathcal{D}_i . Let $p = K/M$. Similar client selection was considered in [1, 2, 33]. Then the adversary adaptively chooses the set $\mathcal{S}_t \subset \tilde{\mathcal{S}}_t$ of participating clients. The adversary's choice of \mathcal{S}_t may depend on the sets of local data points $\{z_{i,\tau} : \tau \leq t, i \in [M]\}$ drawn by all clients up to time t and the sets of participating clients $\{\mathcal{S}_\tau, \tau \leq t-1\}$ chosen previously. We also allow the adversary to have total access to all system parameters including n_i and local objective functions F_i . In other words, the adversary is fully aware of everything that happened up to time t . Such adaptive choice of “faulty” clients is standard in distributed computing literature [11, 12, 17].

To further quantify the degrees of client unavailability, below we impose an upper bound on the total number of data points that are dropped by the adversary at every round t .

Assumption 3.2 (ϵ -adversary dropout fraction).

$$\sum_{i \in \tilde{\mathcal{S}}_t \setminus \mathcal{S}_t} n_i \leq \epsilon \frac{KN}{M}, \quad \forall t.$$

Roughly speaking, since $\mathbb{E} \left[\sum_{i \in \tilde{\mathcal{S}}_t} n_i \right] = KN/M$, Assumption 3.2 says that on average at most ϵ fraction of the sampled data points can be further dropped out by the adversary. In the data

balanced setting where $n_i = N/M$ for all i , Assumption 3.2 simplifies to $|\tilde{\mathcal{S}}_t \setminus \mathcal{S}_t| \leq \epsilon K$, that is, at most ϵ -fraction of clients in $\tilde{\mathcal{S}}_t$ are non-responsive.

We remark that our adversary model covers random unavailability as a special case. With $\epsilon = 0$, our adversary model reduces to the uniform-at-random client unavailability.

4 Algorithms and convergence guarantees

Algorithms. We analyze variants of FedAvg and FedProx in this section. Formally, in each communication round t , each client $i \in \mathcal{S}_t$ updates the model based on the local function $\ell_{i,t}(\theta) \triangleq \frac{1}{n_i} \sum_{j=1}^{n_i} \ell_i(\theta; z_{i,t}^{(j)})$, where $z_{i,t} = (z_{i,t}^{(1)}, \dots, z_{i,t}^{(n_i)})$ is a fresh sample batch of size n_i :

- FedAvg: First, set $\theta_{i,t}^0 = \theta_t$; then perform s local updates as $\theta_{i,t}^{\tau+1} = \theta_{i,t}^\tau - \eta_t \nabla \ell_{i,t}(\theta_{i,t}^\tau)$ for $\tau = 0, \dots, s-1$; finally, set $\theta_{i,t+1} = \theta_{i,t}^s$.
- FedProx¹:

$$\theta_{i,t+1} \in \arg \min_z \tilde{\ell}_{i,t}(z) \triangleq \ell_{i,t}(z) + \frac{1}{2\eta_t} \|z - \theta_t\|_2^2. \quad (2)$$

Upon receiving the local model update $\theta_{i,t+1}$ from active clients in \mathcal{S}_t , the parameter server computes

$$\theta_{t+1} = \theta_t + \beta \sum_{i \in \mathcal{S}_t} w_i (\theta_{i,t+1} - \theta_t), \quad (3)$$

where $\beta \geq 1$ is a parameter introduced to compensate for the lack of participation of the unavailable and non-sampled clients. Note that the standard FedAvg algorithm [1] updates $\theta_{t+1} = \theta_t + \sum_{i \in \mathcal{S}_t} \frac{w_i}{\sum_{j \in \mathcal{S}_t} w_j} (\theta_{i,t+1} - \theta_t)$ and hence can be viewed as a special instance of (3) with varying $\beta = \frac{1}{\sum_{j \in \mathcal{S}_t} w_j}$. However, this choice of β may lead to unstable performance as we observe in numerical experiments.

Assumption 4.1. We assume that

$$\|\nabla \ell_{i,t}(u) - \nabla \ell_{i,t}(v)\|_2 \leq L_i \|u - v\|_2. \quad (4)$$

For FedProx, we additionally assume that

$$\lambda_{\min}(\nabla^2 \ell_{i,t}(\theta)) \geq -L_-, \quad \forall i, \text{ and } \forall t. \quad (5)$$

The conditions are commonly used in the convergence analysis of federated learning algorithms (see e.g. [31, 16]). Define $L \triangleq \max_{i \in [M]} L_i$. Eq. (5) ensures that, using a sufficiently small η_t , the local proximal program (2) in FedProx is strongly convex, and hence the solution can be efficiently computed. Nevertheless, the local objective functions $\ell_{i,t}$ and F_i may still be non-convex.

Let \mathcal{F}_t denote the filtration generated by the sequence $\{z_{i,\tau}, \mathcal{S}_\tau : \tau \leq t-1, i \in [M]\}$. Then $\theta_t \in \mathcal{F}_t$. It follows that $\tilde{\mathcal{S}}_t$ and $z_{i,t}$ for $i \in [M]$ are independent of \mathcal{F}_t .

Assumption 4.2. We assume that

$$\mathbb{E}[\nabla \ell_{i,t}(\theta_t) \mid \mathcal{F}_t] = F_i(\theta_t), \quad (6)$$

$$\mathbb{E}[\|\nabla \ell_{i,t}(\theta_t) - F_i(\theta_t)\|_2^2 \mid \mathcal{F}_t] \leq \sigma_i^2. \quad (7)$$

Let $\sigma^2 = \sum_{i=1}^M w_i \sigma_i^2$ denote the average noise level.

¹We assume the exact minimizer for ease of presentation. Our results can be readily extended when $\theta_{i,t+1}$ is an approximate solution, see e.g., [31, Definition 2] and [16, Definition 3].

4.1 Non-convex functions

Theorem 4.3. Let $F_{\min} \triangleq \inf_{\theta} F(\theta) > -\infty$, Assumptions 3.1–4.2 hold, and $\sqrt{\epsilon}B \leq 0.1$. Let R be the random time with $\mathbb{P}[R = k] = \eta_k / \sum_{t=0}^T \eta_t$ for $k = 0, \dots, T$. For FedAvg, choose $\eta_t \leq \frac{1}{10\beta s LB^2}$ for all t ; For FedProx, choose $\eta_t \leq \frac{1}{10\beta LB^2} \wedge \frac{1}{10L_-}$ for all t . Then, there exists a universal constant c such that

$$\mathbb{E} \|\nabla F(\theta_R)\|_2^2 \leq \frac{3(F(\theta_0) - F_{\min})}{\beta p s \sum_{t=0}^T \eta_t} + \left(4\epsilon + \frac{c\beta s L \sum_{t=0}^T \eta_t^2}{\sum_{t=0}^T \eta_t}\right) (G + \sigma)^2, \quad (8)$$

where $s = 1$ for FedProx. Consequently, let $\hat{\theta} = \theta_R$ with $\sum_{t=0}^T \eta_t \rightarrow \infty$ and $\frac{\sum_{t=0}^T \eta_t^2}{\sum_{t=0}^T \eta_t} \rightarrow 0$. Then,

$$\lim_{T \rightarrow \infty} \mathbb{E} \|\nabla F(\hat{\theta})\|_2^2 \leq 4\epsilon (G + \sigma)^2. \quad (9)$$

Below we show the convergence rates under some concrete schemes of the learning rate based on Theorem 4.3. In the first case, η_t depends on the eventual termination time T , which may be chosen based on a prescribed level of optimality; in the second case, η_t is independent of T , so the program can be executed indefinitely. We only present the results for the FedAvg, and the results for the FedProx are entirely analogous yet with $s = 1$. The proof is deferred to Appendix A. Let $\Delta = F(\theta_0) - F_{\min}$. Recall that $p = K/M$.

Corollary 4.4. For FedAvg: Choose $\eta_t = \frac{1}{10\beta LB^2} \wedge \frac{1}{\beta\sqrt{pTL}(G+\sigma)}$. Then

$$\mathbb{E} \|\nabla F(\theta_R)\|_2^2 \leq \frac{30\Delta LB^2}{psT} + \sqrt{\frac{L}{pT}} (3\Delta + cs)(G + \sigma) + 4\epsilon (G + \sigma)^2.$$

Choose $\eta_t = \frac{\eta_0}{\sqrt{t+1}}$ for all $t \geq 0$, where $\eta_0 = \frac{1}{10\beta LB^2} \wedge \frac{1}{\beta\sqrt{pL}(G+\sigma)}$. Then

$$\mathbb{E} \|\nabla F(\theta_R)\|_2^2 \leq \frac{30\Delta LB^2}{ps\sqrt{T}} + \sqrt{\frac{L}{pT}} (3\Delta + cs \log(e(T+1)))(G + \sigma) + 4\epsilon (G + \sigma)^2.$$

The rate $O(1/\sqrt{T})$ matches that of the standard stochastic gradient descent for optimizing non-convex functions [13]. In fact, the rate $O(1/\sqrt{T})$ is the best possible for any first-order method that has only access to noisy gradients (see e.g. [15, Theorem 3]).

4.2 Strongly convex functions

We say F is μ -strongly convex if

$$\langle \nabla F(x) - \nabla F(y), x - y \rangle \geq \mu \|x - y\|_2^2, \quad \forall x, y. \quad (10)$$

It is worth noting that the convergence results here only require the global objective F to be strongly convex, while we allow non-convex local objective F_i . This is slightly more relaxed compared with the typical assumptions that the local population functions F_i at every client are μ -strongly convex in [3, 32, 7].

Theorem 4.5. Suppose that F is μ -strongly convex and $B\sqrt{\epsilon} < 0.1\frac{\mu}{L}$, and Assumptions 3.1–4.2 hold. Choose $\eta_t = \alpha/(t + \gamma)$, where α, γ are constants such that $\alpha \geq 2/(\beta p s \mu)$, $\alpha/\gamma \leq \frac{\mu}{20\beta L^2 B^2}$, and further $\alpha/\gamma \leq \frac{1}{10L_-}$ for FedProx. Then, there exist some universal constant c ,

$$\begin{aligned} \mathbb{E} \|\theta_t - \theta^*\|_2^2 &\leq \left(1 + \frac{t}{\gamma}\right)^{-1.1} \|\theta_0 - \theta^*\|_2^2 + \frac{4\epsilon}{\mu^2} (G + \sigma)^2 \\ &\quad + \frac{c}{p\mu^2} (G + \sigma)^2 \frac{1}{t + \gamma}. \end{aligned}$$

Note that μ/L is an upper bound to the condition number of Hessian matrix $\nabla^2 F$. Thus, our standing condition $B\sqrt{\epsilon} < 0.1\frac{\mu}{L}$ indicates that a larger fraction of adversarial dropouts can be tolerated when the population function F is better conditioned.

Theorem 4.5 shows that θ_t converges to θ^* at a rate of $O(1/t)$. The $O(1/t)$ convergence rate is the best possible for any first-order method that has only access to noisy gradients [14], [7, Theorem E.1]. When there is no adversarial dropout, our results reduce to the state-of-art convergence results for FedAvg or FedProx. For instance, an exponential decay term similar to $(1 + t/\gamma)^{-1.1} \|\theta_0 - \theta^*\|_2$ and a linear decay term similar to $(\sigma^2 + G^2)/t$ also appear in [32, Theorem V]. The convergence results in [3] are similar but a bit weaker: there is a linear decay term similar to $(\sigma^2 + G^2)/t$, but the error bound decays only linearly rather than exponentially in the initial error as $\|\theta_0 - \theta^*\|_2/t$.

Remark 4.6 (Convex objective functions). Theorem 4.5 establishes the convergence of θ_t to θ^* in the squared L_2 norm for strongly-convex functions F . It is tempting to ask whether we can establish the convergence of $F(\theta_t)$ to $F(\theta^*)$ for convex (but not necessarily strongly-convex) functions F , which is possible for standard stochastic gradient descent without adversarial dropouts (cf. [13, Theorem 2.1]). If we assume, in addition, that $\|\theta_t - \theta^*\|_2$ is always bounded by C , then by convexity of F we can get that

$$F(\theta_t) - F(\theta^*) \leq \langle \nabla F(\theta_t), \theta_t - \theta^* \rangle \leq C \|\nabla F(\theta_t)\|_2,$$

which can be further bounded using the convergence of $\|\nabla F(\theta_t)\|_2$ established in Theorem 4.3. It remains open to establish the convergence for function values for general convex functions without assuming the boundedness of $\|\theta_t - \theta^*\|_2$. The main technical hurdle lies in the fact that the deviations caused by the objective inconsistency and the adversarial selections depend on $\|\theta_t - \theta^*\|_2$, which can be potentially much larger than $\nabla F(\theta_t)$ or $F(\theta_t) - F(\theta^*)$, when F is flat around the minimum point x^* .

5 Proofs of the main convergence guarantees

We provide proof of our main theorems and discuss the connections and differences from existing SGD analysis. The proof focuses on the FedAvg in the general non-convex functions setting. The cases for FedProx or strongly convex functions can be shown via similar arguments and deferred to appendices.

5.1 Key challenges

Recall that each F_i is L_i -smooth. Hence, F is L -smooth with $L = \max_i L_i$ and thus

$$F(\theta_{t+1}) \leq F(\theta_t) + \langle \nabla F(\theta_t), \theta_{t+1} - \theta_t \rangle + \frac{L}{2} \|\theta_{t+1} - \theta_t\|_2^2. \quad (11)$$

The progress over one communication round $\theta_{t+1} - \theta_t$ per aggregation rule (3) is given by $\theta_{t+1} - \theta_t = \beta \sum_{i \in \mathcal{S}_t} w_i (\theta_{i,t+1} - \theta_t)$. The classical SGD iteration relies on the unbiasedness of $\theta_{i,t+1} - \theta_t$ for the direction of $-\nabla F(\theta_t)$. The unbiasedness fails to hold due to the following two reasons:

- **Objective inconsistency.** Under FedAvg or FedProx, the clients either run multiple-step of local SGD or solve a subroutine with proximity regularization. The bias of local updates arises from objective inconsistency or client-drift as analyzed by [34, 32] for FedAvg. Define

$$B_t^{\text{obj}} \triangleq \sum_{i \in \mathcal{S}_t} w_i (\theta_{i,t+1} - \theta_t - (-s\eta_t \nabla \ell_{i,t}(\theta_t))). \quad (12)$$

- **Selection bias.** Given the sampled clients $\tilde{\mathcal{S}}_t$, the non-responsive clients $\tilde{\mathcal{S}}_t \setminus \mathcal{S}_t$ are selected by the system adversary; consequently, the resulting participating clients \mathcal{S}_t no longer form a representative subset of all clients. What's more, the adversarial selection is time-varying and may even be *correlated* with the data used to evaluate the local gradients. Define

$$B_t^{\text{sel}} \triangleq \sum_{i \in \tilde{\mathcal{S}}_t \setminus \mathcal{S}_t} w_i \nabla \ell_{i,t}(\theta_t).$$

Our simple variants of FedAvg and FedProx can provably control the biases stemming from the two sources identified above. Existing bias reduction methodologies such as those proposed by [34, 32] only address the issue of objective inconsistency.

5.2 Objective inconsistency

We first introduce some convenient notations for the local update rules for FedAvg. Let $\mathcal{G}_{i,t}(\theta; \eta)$ denote the mapping of the gradient descent on client i in round t with the learning rate η :

$$\mathcal{G}_{i,t}(\theta; \eta) \triangleq \theta - \eta \nabla \ell_{i,t}(\theta). \quad (13)$$

Then, the locally updated model after s steps of gradient descent is $\theta_{i,t+1} = \mathcal{G}_{i,t}^s(\theta_t, \eta_t)$, where

$$\mathcal{G}_{i,t}^s(\cdot; \eta) \triangleq \underbrace{\mathcal{G}_{i,t}(\cdot; \eta) \circ \cdots \circ \mathcal{G}_{i,t}(\cdot; \eta)}_{s \text{ times}}.$$

After collecting the updated model $\theta_{i,t+1}$ for $i \in \mathcal{S}_t$, PS aggregates the local updates via (3).

Choosing a large s accelerates the training process. However, it also increases the deviation from the stochastic gradient quantified in (12), and possibly renders training process unstable as observed in [1]. To quantify the stability of multiple local gradient steps, define

$$\kappa \triangleq \max_{i,t} \frac{(1 + \eta_t L_i)^s - 1 - s\eta_t L_i}{\binom{s}{2} (\eta_t L_i)^2}.$$

Intuitively, κ characterizes the deviation of multiple local gradient descent from a single gradient descent with a larger step size, as shown in Lemma 5.1. For the special case that $s = 1$, we have $\kappa = 0$; for $s \geq 2$, it always holds that $\kappa \geq 1$. Furthermore, $\kappa \leq \frac{e^c - 1 - c}{c^2/2}$ if $\eta_t \leq \frac{c}{sL}$. We have the following lemma, which upper-bounds the deviation from the desired direction uniformly for all θ .

Lemma 5.1. *For $s \geq 1$, we have*

$$\|\theta - \mathcal{G}_{i,t}^s(\theta; \eta_t) - s\eta_t \nabla \ell_{i,t}(\theta)\|_2 \leq \kappa \eta_t^2 \binom{s}{2} L_i \|\nabla \ell_{i,t}(\theta)\|_2, \quad \forall \theta.$$

With Lemma 5.1, we can now bound the bias due to objective inconsistency as follows:

$$\begin{aligned}
\|B_t^{\text{obj}}\|_2 &= \left\| \sum_{i \in \mathcal{S}_t} w_i (\mathcal{G}_{i,t}^s(\theta_t; \eta_t) - \theta_t + s\eta_t \nabla \ell_{i,t}(\theta_t)) \right\|_2 \\
&\leq \sum_{i \in \mathcal{S}_t} w_i \|\mathcal{G}_{i,t}^s(\theta_t; \eta) - \theta_t + s\eta_t \nabla \ell_{i,t}(\theta_t)\|_2 \\
&\stackrel{(a)}{\leq} \kappa \eta_t^2 L \binom{s}{2} \sum_{i \in \mathcal{S}_t} w_i \|\nabla \ell_{i,t}(\theta_t)\|_2 \stackrel{(b)}{\leq} \kappa \eta_t^2 L \binom{s}{2} \sum_{i \in \tilde{\mathcal{S}}_t} w_i \|\nabla \ell_{i,t}(\theta_t)\|_2,
\end{aligned}$$

where inequality (a) holds from Lemma 5.1 and inequality (b) is true because that $\mathcal{S}_t \subseteq \tilde{\mathcal{S}}_t$.

Note that

$$\mathbb{E} \left[\sum_{i \in \tilde{\mathcal{S}}_t} w_i \|\nabla \ell_{i,t}(\theta_t)\|_2 \mid \mathcal{F}_t \right] \leq \mathbb{E} \left[\sum_{i \in \tilde{\mathcal{S}}_t} w_i \|\nabla F_i(\theta_t)\|_2 \mid \mathcal{F}_t \right] + \mathbb{E} \left[\sum_{i \in \tilde{\mathcal{S}}_t} w_i \|\nabla \ell_{i,t}(\theta_t) - \nabla F_i(\theta_t)\|_2 \mid \mathcal{F}_t \right]. \quad (14)$$

It remains to bound the two terms in the RHS of (14) separately. First, we have

$$\begin{aligned}
\mathbb{E} \left[\sum_{i \in \tilde{\mathcal{S}}_t} w_i \|\nabla F_i(\theta_t)\|_2 \mid \mathcal{F}_t \right] &= \mathbb{E} \left[\sum_{i=1}^M w_i \|\nabla F_i(\theta_t)\|_2 \mathbf{1}_{\{i \in \tilde{\mathcal{S}}_t\}} \mid \mathcal{F}_t \right] \\
&\stackrel{(a)}{=} p \sum_{i \in [M]} w_i \|\nabla F_i(\theta_t)\|_2 \\
&\stackrel{(b)}{\leq} p \sqrt{\sum_{i \in [M]} w_i \|\nabla F_i(\theta_t)\|_2^2} \\
&\stackrel{(c)}{\leq} p \sqrt{B^2 \|\nabla F(\theta_t)\|_2^2 + G^2} \\
&\leq p (B \|\nabla F(\theta_t)\|_2 + G), \quad (15)
\end{aligned}$$

where equality (a) is true by the independent between $\tilde{\mathcal{S}}_t$ and \mathcal{F}_t ; inequality (b) holds by Jensen's inequality; inequality (c) follows from Assumption 3.1. Analogously,

$$\begin{aligned}
\mathbb{E} \left[\sum_{i \in \tilde{\mathcal{S}}_t} w_i \|\nabla \ell_{i,t}(\theta_t) - \nabla F_i(\theta_t)\|_2 \mid \mathcal{F}_t \right] &= p \sum_{i \in [M]} w_i \mathbb{E} [\|\nabla \ell_{i,t}(\theta_t) - \nabla F_i(\theta_t)\|_2 \mid \mathcal{F}_t] \\
&\stackrel{(a)}{\leq} p \sqrt{\sum_{i \in [M]} w_i \mathbb{E} [\|\nabla \ell_{i,t}(\theta_t) - \nabla F_i(\theta_t)\|_2^2 \mid \mathcal{F}_t]} \\
&\stackrel{(b)}{\leq} p \sqrt{\sum_{i \in [M]} w_i \sigma_i^2} = p\sigma, \quad (16)
\end{aligned}$$

where inequality (a) is true by applying Jensen's inequality twice, and inequality (b) follows from (7). Combining (14), (15), and (16), we get

$$\mathbb{E} \left[\sum_{i \in \tilde{\mathcal{S}}_t} w_i \|\nabla \ell_{i,t}(\theta_t)\|_2 \mid \mathcal{F}_t \right] \leq p (B \|\nabla F(\theta_t)\|_2 + G + \sigma). \quad (17)$$

Therefore,

$$\mathbb{E} \left[\left\| B_t^{\text{obj}} \right\|_2 \mid \mathcal{F}_t \right] \leq p\kappa\eta_t^2 L \binom{s}{2} (B \|\nabla F(\theta_t)\|_2 + G + \sigma). \quad (18)$$

5.3 Selection bias

Since \mathcal{S}_t is time-varying and is correlated with $\nabla \ell_{i,t}(\theta_t)$, we upper-bound the selection bias *uniformly* via the analysis of extreme values. Two main ingredients in our analysis are: 1) the power of the adversary is limited as specified by Assumption 3.2; 2) the dissimilarity among the clients is bounded given by Assumption 3.1.

Lemma 5.2. *Under Assumptions 3.1 and 3.2, we have*

$$\mathbb{E} \left[\left\| \sum_{i \in \tilde{\mathcal{S}}_t \setminus \mathcal{S}_t} w_i \nabla \ell_{i,t}(\theta_t) \right\|_2 \mid \mathcal{F}_t \right] \leq p\sqrt{\epsilon} (B \|\nabla F(\theta_t)\|_2 + G + \sigma). \quad (19)$$

The above lemma gives an upper bound to $\mathbb{E} [\|B_t^{\text{sel}}\|_2 \mid \mathcal{F}_t]$. Surprisingly, ϵ -fraction of maliciously chosen unavailable clients can contribute a deviation of $O(\sqrt{\epsilon})$. The rate turns out to be optimal as the estimation error matches the fundamental limit in Theorem 6.1.

5.4 Combining together

Once we have tight upper bounds on the bias, the remaining steps are mostly similar to the standard SGD analysis. Specifically,

$$\begin{aligned} \theta_{t+1} - \theta_t &= \beta \sum_{i \in \mathcal{S}_t} w_i (\theta_{i,t+1} - \theta_t) = -\beta s \eta_t \sum_{i \in \mathcal{S}_t} w_i \nabla \ell_{i,t}(\theta_t) + \beta B_t^{\text{obj}} \\ &= -\beta s \eta_t \sum_{i \in \tilde{\mathcal{S}}_t} w_i \nabla \ell_{i,t}(\theta_t) + \beta B_t^{\text{obj}} + \beta s \eta_t B_t^{\text{sel}}, \end{aligned}$$

where $\mathbb{E}[\|B_t^{\text{obj}}\|_2 \mid \mathcal{F}_t]$ and $\mathbb{E}[\|B_t^{\text{sel}}\|_2 \mid \mathcal{F}_t]$ are upper bounded by (18) and (19), respectively.

For the first term, recall that \mathcal{S}_t is the set of the K clients randomly sampled at round t . Since θ_t is adapted to \mathcal{F}_t , we have

$$\begin{aligned} \mathbb{E} \left[\sum_{i \in \tilde{\mathcal{S}}_t} w_i \nabla \ell_{i,t}(\theta_t) \mid \mathcal{F}_t \right] &= \mathbb{E} \left[\sum_{i=1}^M w_i \nabla \ell_{i,t}(\theta_t) \mathbf{1}_{\{i \in \tilde{\mathcal{S}}_t\}} \mid \mathcal{F}_t \right] \\ &\stackrel{(a)}{=} \sum_{i=1}^M w_i \mathbb{E} [\nabla \ell_{i,t}(\theta_t) \mid \mathcal{F}_t] \mathbb{E} [\mathbf{1}_{\{i \in \tilde{\mathcal{S}}_t\}} \mid \mathcal{F}_t] \\ &\stackrel{(b)}{=} \sum_{i=1}^M w_i \nabla F_i(\theta_t) p \stackrel{(c)}{=} p \nabla F(\theta_t), \end{aligned} \quad (20)$$

where (a) holds because $\tilde{\mathcal{S}}_t \perp\!\!\!\perp z_{i,t} \mid \mathcal{F}_t$; (b) follows from the sampling fraction $\mathbb{E} [\mathbf{1}_{\{i \in \tilde{\mathcal{S}}_t\}} \mid \mathcal{F}_t] = K/M = p$; (c) applies (6).

Applying the above analysis in (11), we obtain the progress in one communication round, which further yields upper bounds of $\|\nabla F(\theta_t)\|_2$ via suitable scheduling of learning rates and a telescoping sum over the iterations. See details in Appendix B.1.

6 Minimax lower bounds

In this section, we prove a minimax lower bound on the estimation error rates.

Theorem 6.1. *Given any algorithm (including randomized and non-FL algorithm) and any time horizon T (including $T = \infty$), there always exists a choice of M functions $\{\ell_{i,t}(\theta) : i \in [M], t \in [T]\}$ for which*

- *each $\ell_{i,t}$ is L -smooth and μ -strongly convex;*
- *$F_i(\theta) \triangleq \mathbb{E}[\ell_{i,t}(\theta)]$ satisfies the (B, G) condition;*
- *$\text{var}(\nabla \ell_{i,t}(\theta)) \leq \sigma_i^2$,*

and a choice of $\mathcal{S}_t \subset [M]$ for $t \in [T]$ with $|\mathcal{S}_t| \geq (1 - \epsilon)M$ such that the output of the algorithm $\hat{\theta}$ given access to $\{\ell_{i,t}(\theta) : i \in \mathcal{S}_t, t \in [T]\}$ has an error at least

$$\mathbb{E} \left[\|\nabla F(\hat{\theta})\|^2 \right] \geq \frac{\epsilon}{8(1 - \epsilon)} (G^2 + \sigma^2), \quad (21)$$

when F is non-convex;

$$\mathbb{E} \left[\|\hat{\theta} - \theta^*\|_2^2 \right] \geq \frac{\epsilon}{8(1 - \epsilon)\mu^2} (G^2 + \sigma^2), \quad (22)$$

when F is μ -strongly convex.

We have shown in Theorems 4.3 and 4.5 that the lower bounds in (21) and (22) can be attained (up to a constant factor) by simple variants of the standard FedAvg and FedProx with only access to noisy gradients and even when the adversary can adaptively choose \mathcal{S}_t based on all the history information.

6.1 Proof sketch and comparison of lower bounds

To deduce that the lower bounds are at least on the order of ϵG^2 , it suffices to construct time-invariant \mathcal{S}_t . We construct two instances: one homogeneous instance where $\ell_{i,t} = f$ for all i, t ; and the other heterogeneous instance where $\ell_{i,t} = f$ for $i \in S$ and $\ell_{i,t} = g$ for $i \notin S$ for a fixed subset $S \subset [M]$ with $|S| = (1 - \epsilon)M$. The functions f and g are properly chosen to be sufficiently distinct while satisfying the (B, G) -condition. Importantly, if the adversary chooses $\mathcal{S}_t = S$ for all t , then any algorithm with access to $\{\ell_{i,t} : i \in \mathcal{S}_t\}$ cannot distinguish the two instances and hence cannot simultaneously optimize both instances.

In contrast, to prove the lower bounds on the order of $\epsilon \sigma^2$, it is crucial to have \mathcal{S}_t be time-varying and chosen based on the realization of $\{\ell_{i,t}, i \in [M]\}$. In particular, we again construct two instances. The first instance is exactly the same as before. The second instance replaces S by \mathcal{S}_t chosen uniformly and independently from all subsets of $[M]$ with size $(1 - \epsilon)M$. This time the functions f and g are chosen to be sufficiently distinct while the variance of $\nabla \ell_{i,t}$ is kept at most σ^2 .

Note that the previous work [27] assumes the adversary is static and chooses a prefixed \mathcal{S} to inject errors; thus the lower bound [27, Theorem III] does not contain the $\epsilon \sigma^2$ term as we do. For this reason, when $G = 0$ they show that an FL algorithm with a robust aggregator of noisy gradients can approach the zero optimization error as $T \rightarrow \infty$. However, this is fundamentally impossible in our setting with non-static adversarial dropouts.

Remark 6.2 (The impact of dissimilarity parameter B). The lower bounds in Theorem 6.1 do not depend on the other dissimilarity parameter B . From the analysis of our algorithm, the parameter B in Assumption 3.1 instead influences the convergence speed and the requirement on the learning rate; the eventual precision is unaffected.

Remark 6.3 (Convergence rate in T). Our lower bounds do not capture the dependency on T . It is known in the literature that even in the centralized homogeneous setting, any algorithm with access to T queries of noisy gradients of F with variance σ^2 has to suffer an estimation error $\mathbb{E} [\|\nabla F(\hat{\theta})\|_2^2] \geq \Omega(\sigma/\sqrt{T})$ for non-convex F and $\mathbb{E} [\|\hat{\theta} - \theta^*\|^2] \geq \Omega(\mu^2\sigma^2/T)$ for μ -strongly convex F in the worst case (see e.g., [15, Theorem 3] and [7, Theorem E.1]).

7 Numerical Experiments

In this section, we use numerical experiments to corroborate our theories and analysis on both real-world and synthetic datasets. We evaluate the top-1 accuracy of the proposed variants of FedAvg and FedProx on real-world datasets CIFAR-10 [35], Shakespeare [1], and synthetic dataset following [36, 31].

Baselines. Each of the evaluations consists of two parts:

- (1) Comparisons with the baselines FedAvg [1], FedProx [31], and MIFA [7]. The baseline MIFA is chosen because it is designed against general client unavailability that does not have benign random patterns. The key idea of MIFA is that for unavailable clients, the parameter server uses the memorized latest updates from those clients for aggregation. For clients running FedProx, we use momentum SGD to solve the local program. For ease of presentation, henceforth we refer to FedAvg, MIFA, and our FedAvg variant as FedAvg-type algorithms because that the clients under those algorithms share the same form of local computations.
- (2) Comparisons with the Byzantine-resilient algorithms centered clipping (cclip) [26], geometric median (GM) [22], and their bucketing variants [27]. Given $\{x_1, \dots, x_M\} \subseteq \mathbb{R}^d$, cclip [26] and GM [22] aggregate those M points as follows:

- cclip: Given the clipping radius $\tau > 0$ and iteration budget L , $\text{agg}_{\text{cclip}, L}(x_1, \dots, x_M)$ is iteratively obtained as

$$v_{\ell+1} = v_\ell + \frac{1}{M} \sum_{i=1}^M (x_i - v_\ell) \min \left\{ 1, \frac{\tau}{\|x_i - v_\ell\|_2} \right\} \quad \text{for } \ell = 0, \dots, L-1.$$

In our experiments, we choose $L = 3$, the same as in [26], and an initial guess $v_0 = \mathbf{0}$.

- GM: $\text{agg}_{\text{GM}}(x_1, \dots, x_M) \triangleq \arg \min_{v \in \mathbb{R}^d} \sum_{i=1}^M \|v - x_i\|_2$.
In our experiments, we use the smoothed Weiszfeld algorithm (Algorithm 2 in [37]) with iteration budget $R = 8$, which finds an approximate minimizer of $\min_{v \in \mathbb{R}^d} \sum_{i=1}^M \|v - x_i\|_2$.
- Bucketing is a technique that aims to reduce the impact of data heterogeneity. It randomly partitions the M points into $\lceil M/(bs) \rceil$ buckets for some tuning parameter bs that determines the bucket size. Then, the data points in each bucket are averaged to construct bucket means $\hat{x}_1, \dots, \hat{x}_{\lceil M/(bs) \rceil}$, which are fed into aggregators such as cclip and GM.

Following [27, Section 5], we use momentum for the Byzantine-resilient algorithms to reduce the variance of the stochastic gradients. That is, the $\{x_1, \dots, x_M\}$ are the local momentum of the cumulative stochastic gradients. To account for partial client participation, for the inactive

clients, the parameter server reuses their local momentum in the last active rounds, analogously to MIFA, for a fair comparison. Similar to [27], we set the bucket size $bs = 2$.

Setup and hyperparameters. For CIFAR-10 and synthetic datasets, we let the datasets be distributed over $M = 100$ clients. In each round, $K = 10$ clients are sampled uniformly at random without replacement to build $\tilde{\mathcal{S}}_t$. The data partition and client population are a bit different for Shakespeare dataset; see Section 7.3 for details.

For our algorithms, the amplification factor β is set as $M/K = 10$ throughout. The learning rates and the proximal coefficient are tuned from grid searches, where the initial learning rates $\eta_0 \in \{10^{-4}, \dots, 10^1\}$, but the proximal coefficient $\mu_t \triangleq (1/\eta_t) \in \{10^{-3}, \dots, 1\}$ in Eq. (2). In our experiments, we choose $\mu_t = \mu_0 = (1/\eta_0)$. Notably, we run SGD with momentum as Eq. (23) on each client i to solve the local program of FedProx and Byzantine-resilient algorithms:

$$\begin{cases} m_{i,t}^{\tau+1} = \beta_0 m_{i,t}^\tau + (1 - \beta_0) \nabla \ell_{i,t}(\theta_{i,t}^\tau) \\ \theta_{i,t}^{\tau+1} = \theta_{i,t}^\tau - \alpha_0 m_{i,t}^\tau, \end{cases} \quad (23)$$

where $\theta_{i,t}^\tau$ denotes the updated model after τ steps local computations in round t on client i with $\theta_{i,t} = \theta_t$ for all $i \in [M]$ and $t \geq 0$. A common practice $\beta_0 = 0.9$ is adopted as the momentum coefficient and fixes a constant local learning rate α_0 tuned from the same grid as η_0 . For a constant learning rate, we consider $\eta_t = \eta_0$ for all $t \geq 0$. For a decaying learning rate, let $\eta_t = \eta_0 / \sqrt{t + 1}$.

The hyper-parameter setups are summarized in Table 1. Additional details of the experiments and hardware environments are deferred to Appendix C.

Dataset	Algorithms	Learning Rates	Initial Rates	Local Solver	Local Steps	Batch Size
CIFAR-10	FedAvg-type	$\eta_0 / \sqrt{t + 1}$	$\eta_0 = 0.1$	SGD	$s = 25$	100
	FedProx, FedProx variant	α_0	$\alpha_0 = 0.03, \mu_0 = 0.1$	SGD with momentum	$s = 10$	
	GM, cclip, and their bucketing variants	α_0	$\alpha_0 = 0.001$	SGD with momentum	$s = 1$	
Shakespeare	FedAvg-type	$\eta_0 / \sqrt{t + 1}$	$\eta_0 = 1$	SGD	$s = 200$	500
	GM, cclip, and their bucketing variants	α_0	$\alpha_0 = 0.8$	SGD with momentum	$s = 1$	
Synthetic	FedAvg-type	η_0	$\eta_0 = 0.01$	SGD	$s = 25$	Full batch
	FedProx, FedProx variant	α_0	$\alpha_0 = 0.01, \mu_0 = 1$	SGD with momentum	$s = 10$	
	GM, cclip, and their bucketing variants	α_0	$\alpha_0 = 0.01$	SGD with momentum	$s = 1$	

Table 1: Hyper-parameter setups

7.1 Adversarial client unavailability scheme

In this subsection, we describe our client unavailability scheme for the system adversary. Additional adversarial client unavailability schemes can be found in Appendix C.3.

Our adversarial client unavailability scheme entails the selection of specific clients from $\tilde{\mathcal{S}}_t$ to dropout. The high-level idea is to have the adversary drop the most valuable clients. To assess the value of a client, we consider the difference of gradients between a pair of rounds T_1, T_2 , which can be further tuned. In fact, our scheme can be readily extended to multiple pairs of such round indices. Specifically, the adversary excludes the clients whose gradients change the most significantly between two chosen communication rounds. A key obstacle in exactly realizing this scheme is that the system adversary has no future information which is required to compute the aforementioned gradient changes. To get around this, we use auxiliary experiments and leverage the knowledge of the clients' local data distribution to obtain an approximation of the gradient changes.

Next we provide details of our approximation. Before running regular experiments, the adversary conducts independent runs of FedAvg and cclip with full client participation. The local

datasets in these auxiliary experiments are independent copies of those in regular experiments, which both follow the same local distribution and thus can be achieved through the use of distinct random seeds. We denote the auxiliary local objective function as $\tilde{\ell}_{i,t}$, the auxiliary local model obtained from FedAvg after τ steps as $\tilde{\theta}_{i,t}^\tau$, and the auxiliary local momentum vector from cclip as $\tilde{m}_{i,t}$ for $i \in [M]$ and $t \geq 0$. For two carefully chosen rounds T_1 and T_2 , we compute the gradient norm $g_{i,t} \triangleq \|\sum_{\tau=0}^{s-1} \nabla \tilde{\ell}_{i,t}(\tilde{\theta}_{i,t}^\tau)\|_2$, and the momentum norm $g'_{i,t} \triangleq \|\tilde{m}_{i,t}\|_2$ for $t \in \{T_1, T_2\}$. We construct set \mathcal{C} , termed as *candidate set of valuable clients*, as follows:

1. $\mathcal{C}_1 \subseteq [M]$ is a set of K_1 clients such that $|g_{i,T_2} - g_{i,T_1}| \geq |g_{i',T_2} - g_{i',T_1}|$ for $i \in \mathcal{C}_1$ and $i' \in [M] \setminus \mathcal{C}_1$.
2. $\mathcal{C}_2 \subseteq [M] \setminus \mathcal{C}_1$ is a set of K_2 clients such that $|g'_{i,T_2} - g'_{i,T_1}| \geq |g'_{i',T_2} - g'_{i',T_1}|$ for $i \in \mathcal{C}_2$ and $i' \in [M] \setminus (\mathcal{C}_1 \cup \mathcal{C}_2)$.
3. $\mathcal{C} = \mathcal{C}_1 \cup \mathcal{C}_2$.

In our implementation, we set $T_1 = 5$, $T_2 = 150$, $K_1 = 25$, and $K_2 = 10$.

During the execution of the regular experiments, the adversary chooses \mathcal{S}_t by rendering clients in $\mathcal{C} \cap \tilde{\mathcal{S}}_t$ non-responsive subject to the constraint in Assumption 3.2. In particular, in each communication round t , let $(i_{t,1}, \dots, i_{t,K})$ denote the client indices in $\tilde{\mathcal{S}}_t$ after random permutation. Let \mathcal{S}_t be initialized as $\tilde{\mathcal{S}}_t$, and we iteratively select the non-responsive clients. For $k = 1, \dots, K$, if $i_{t,k} \in \mathcal{C}$ and $\sum_{i \in (\tilde{\mathcal{S}}_t \setminus \mathcal{S}_t) \cup \{i_{t,k}\}} n_i \leq \epsilon KN/M$, then set $\mathcal{S}_t \leftarrow \mathcal{S}_t \setminus \{i_{t,k}\}$. The procedure is terminated if $|\mathcal{S}_t| = 1$ to ensure that at least one client is responsive.

Clearly, the above scheme does not use future information from regular experiments.

7.2 Experiments on CIFAR-10

Following [38], the CIFAR-10 dataset is partitioned to build each client's local datasets according to the Dirichlet allocation with parameter α ; the smaller α , the more non-IID of the local data. Each client keeps 500 samples. In each round, client i draws a batch of $n_i \equiv 100$ samples from its local dataset. We choose $\alpha = 0.1$, which creates highly non-IID local datasets due to label skewness, where the volume of each label on the clients is shown in Fig. 1. Dirichlet distribution is commonly adopted for characterizing non-IID distributions (see, e.g., [34, 6, 39]). Notably, $\alpha = 0.1$ was also chosen in [34], $\alpha = 0.5$ was used in [39], and $\alpha \in \{2, 0.3\}$ were considered in [6]. In the plot, we can readily see that the categorical distributions among clients are drastically different. For example, in Fig. 1, client # 1 has five classes of data, whereas client # 100 has three classes. Moreover, the fractions of the classes vary significantly across clients.

We present the results with $\epsilon = 0.8$ in this subsection. The results with other choices of ϵ are similar and are reported in Appendix C. We use LeNet-5 [40] with cross-entropy loss as the network model. We plot the training and test performances every 15 communication rounds.

We observe from Fig. 2 that the proposed variants of FedAvg and FedProx outperform all the other baselines. Compared with the FedAvg and FedProx, our variants progress smoother, and the improvements are quite prominent. Notably, MIFA acts better than FedAvg but falls behind our variants. On the other hand, the Byzantine-resilient algorithms lag behind the proposed algorithms significantly. Detailed discussions on existing Byzantine-resilient algorithms are presented in Section 2.

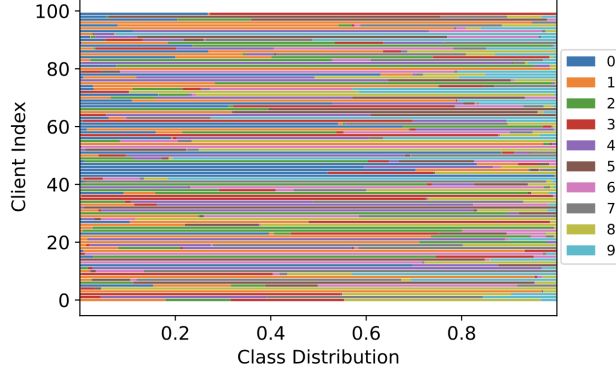


Figure 1: Populations generated from Dirichlet distribution ($\alpha = 0.1$) with different number of clients. Each row corresponds to the empirical distribution of local data in terms of classes. The colors correspond to data with different class labels.

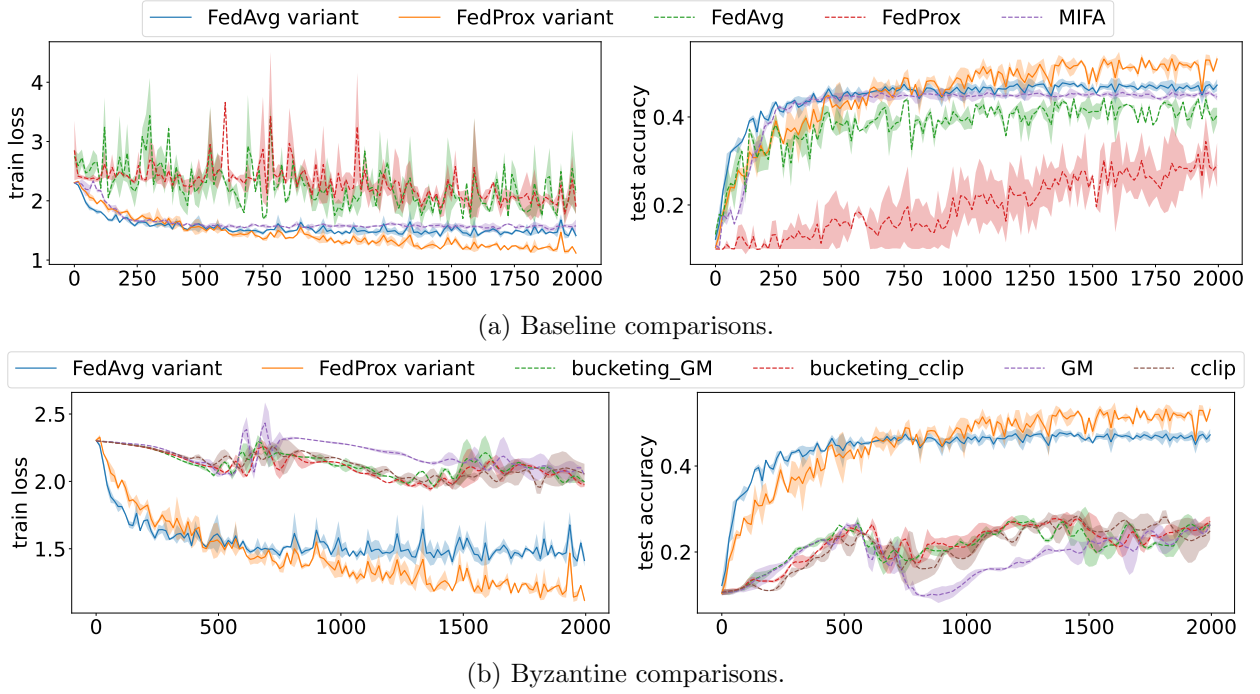


Figure 2: CIFAR-10 results with Dirichlet parameter $\alpha = 0.1$ and dropout fraction $\epsilon = 0.8$ on adversarial client unavailability scheme in Section 7.1.

7.3 Natural language processing (NLP) task: Shakespeare next-character prediction.

We also test the performance of FedAvg-type algorithms on Natural language processing (NLP) task. Our results are presented in Fig. 3. The Shakespeare dataset is built from *The Complete Works of William Shakespeare* [1], which contains 4,226,158 data instances. LEAF [41] (a federated learning benchmark) partitioned it into 660 groups. We sample around 18% from the 660 groups to obtain the local datasets for $M = 125$ clients. The network model is an LSTM network with two layers, each of which has 256 neurons; this model takes in each character as an 8-dimensional embedding. In each round, $K = 20$ clients are sampled to form \tilde{S}_t , and each sampled client draws

a batch of $n_i \equiv 500$ samples. We choose the dropout threshold $\epsilon = 0.7$.

In addition to changing the learning task from computer vision to NLP, we also test a different dropout scheme:

- The adversary calculate the l_2 norms of the local gradient improvement $\|w_i \sum_{\tau=0}^{s-1} \nabla \ell_{i,\tau}\|_2$ at the client $i \in \tilde{\mathcal{S}}_t$ and sort the norms in descending order.
- The adversary inspects clients' data volume n_i for $i \in \tilde{\mathcal{S}}_t$ in the sorted order. If $n_i > \epsilon(KN)/M$, client i will be admitted to the set \mathcal{S}_t . Otherwise, the client's application will be denied until $\sum_{i \in \tilde{\mathcal{S}}_t \setminus \mathcal{S}_t} n_i \leq \epsilon(KN)/M$.

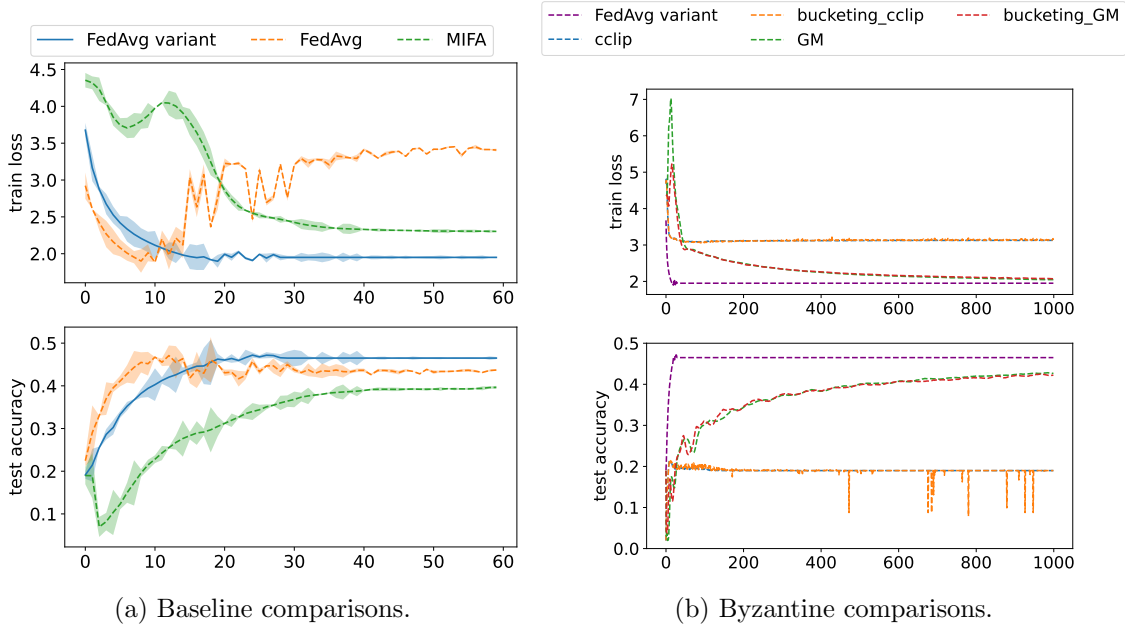


Figure 3: Natural language processing task with dropout fraction $\epsilon = 0.7$ on a different adversarial client unavailability scheme, where the adversary inspects each client's local gradient improvement and removes clients of the greatest improvements subject to Assumption 3.2. Details can be found in Section 7.3.

Intuitively, we discard the most "important" local gradient improvements in terms of l_2 norm.

In Fig. 3a, our FedAvg variant progresses the most smoothly during training and obtains the best results. One can see that the convergence time in Fig. 3a (around 60 rounds) and Fig. 3b (around 1000 rounds) do not match each other. This is because GM and the bucketing version of GM converge very slowly. In both Fig. 3a and Fig. 3b, our FedAvg variant stands as the best.

7.4 Experiments on synthetic datasets

We follow the setup of the synthetic experiments in [36, 31]. We generate the local dataset $(x_{ij}, y_{ij})_{j=1}^{n_i}$ for each client i according to the model $y_{ij} = \arg \max(\text{softmax}(W_i x_{ij} + b_i))$, where $x_{ij} \in \mathbb{R}^{60}$, $W_i \in \mathbb{R}^{10 \times 60}$, $b_i \in \mathbb{R}^{10}$. To generate heterogeneous clients, each element of W_i and b_i is independently drawn from $\mathcal{N}(u_i, 1)$, where $u_i \sim \mathcal{N}(0, 1)$. Moreover, $x_{ij} \sim \mathcal{N}(v_i, \Sigma)$, where the covariance matrix is diagonal with $\sum_{j,j} = j^{-1.2}$. Each element of the mean vector v_i is independently drawn from $\mathcal{N}(B_i, 1)$, where $B_i \sim \mathcal{N}(0, 1)$. In contrast to the experiments on CIFAR-10,

here we consider the setup with quantity skewness, where the local data volume n_i follows a power law as shown in Fig. 4. In the experiments, we run multinomial logistic regression with full batch gradient descent and cross-entropy loss.

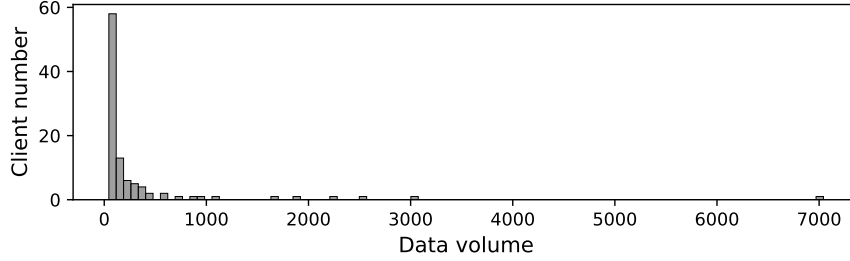


Figure 4: Synthetic datasets: clients’ local data volume histogram.

The first row of Fig. 5 shows the comparisons with the baselines. MIFA’s curve suffers from high fluctuations and does not converge till the end of training. We plot in the second row the comparisons without MIFA. The performances of our variants are similar when compared with the FedAvg and FedProx. Due to the quantity skewness, the actual dropout fraction also fluctuates, and it is possible that no client is dropped in one round. We plot in the third row $\epsilon_t \triangleq (\sum_{i \in \tilde{\mathcal{S}}_t \setminus \mathcal{S}_t} n_i) / (KN/M)$. Nevertheless, our unavailability scheme ensures that $\max_{t \in [T]} \epsilon_t \leq \epsilon$. Additional results with other choices of ϵ are similar and are reported in Appendix C. Similarly, we observe in Fig. 6 that the fluctuations of the Byzantine-resilient algorithms are also severe.

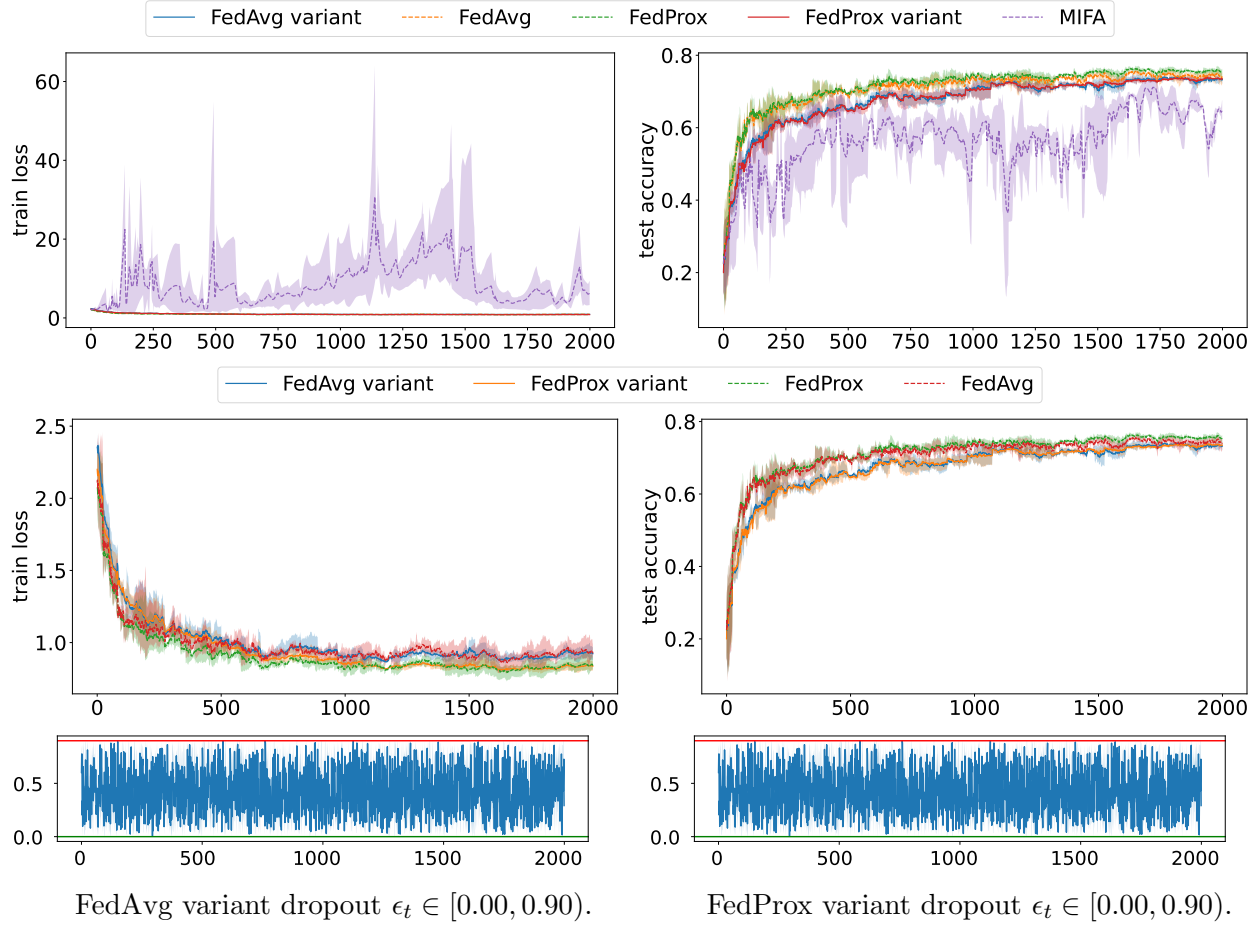


Figure 5: Synthetic datasets: comparisons with baselines with dropout fraction $\epsilon = 0.9$ on adversarial client unavailability scheme in Section 7.1.

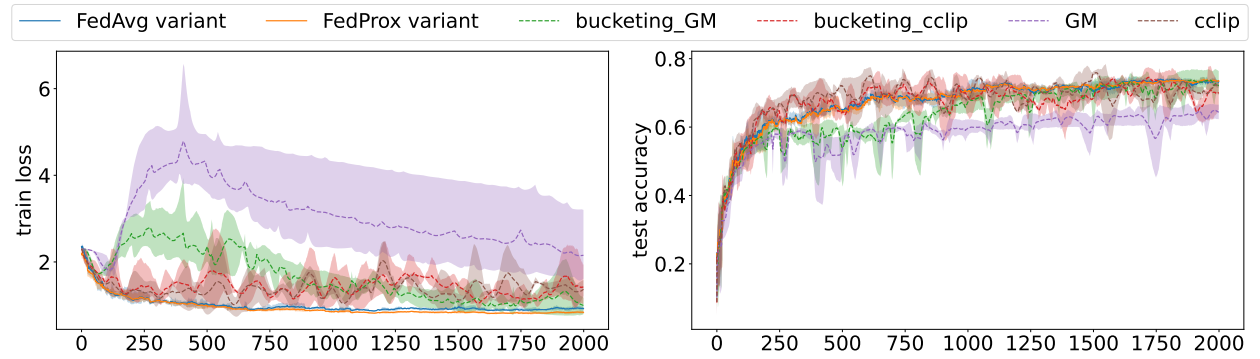


Figure 6: Synthetic datasets: comparisons with Byzantine-resilient algorithms with dropout fraction $\epsilon = 0.9$ on adversarial client unavailability scheme in Section 7.1.

References

- [1] B. McMahan, E. Moore, D. Ramage, S. Hampson, and B. A. y Arcas, “Communication-efficient learning of deep networks from decentralized data,” in *Artificial intelligence and statistics*. PMLR, 2017, pp. 1273–1282.
- [2] P. Kairouz, H. B. McMahan, B. Avent, A. Bellet, M. Bennis, A. N. Bhagoji, K. Bonawitz, Z. Charles, G. Cormode, R. Cummings, R. G. L. D’Oliveira, H. Eichner, S. E. Rouayheb, D. Evans, J. Gardner, Z. Garrett, A. Gascón, B. Ghazi, P. B. Gibbons, M. Gruteser, Z. Harchaoui, C. He, L. He, Z. Huo, B. Hutchinson, J. Hsu, M. Jaggi, T. Javidi, G. Joshi, M. Khodak, J. Konecný, A. Korolova, F. Koushanfar, S. Koyejo, T. Lepoint, Y. Liu, P. Mittal, M. Mohri, R. Nock, A. Özgür, R. Pagh, H. Qi, D. Ramage, R. Raskar, M. Raykova, D. Song, W. Song, S. U. Stich, Z. Sun, A. T. Suresh, F. Tramèr, P. Vepakomma, J. Wang, L. Xiong, Z. Xu, Q. Yang, F. X. Yu, H. Yu, and S. Zhao, “Advances and open problems in federated learning,” *Foundations and Trends® in Machine Learning*, vol. 14, no. 1–2, pp. 1–210, 2021.
- [3] X. Li, K. Huang, W. Yang, S. Wang, and Z. Zhang, “On the convergence of fedavg on non-iid data,” in *International Conference on Learning Representations*, 2020. [Online]. Available: <https://openreview.net/forum?id=HJxNAnVtDS>
- [4] Y. Ruan, X. Zhang, S.-C. Liang, and C. Joe-Wong, “Towards flexible device participation in federated learning,” in *International Conference on Artificial Intelligence and Statistics*. PMLR, 2021, pp. 3403–3411.
- [5] C. Philippenko and A. Dieuleveut, “Bidirectional compression in heterogeneous settings for distributed or federated learning with partial participation: tight convergence guarantees,” *arXiv preprint arXiv:2006.14591*, 2020.
- [6] Y. J. Cho, J. Wang, and G. Joshi, “Towards understanding biased client selection in federated learning,” in *International Conference on Artificial Intelligence and Statistics*. PMLR, 2022, pp. 10 351–10 375.
- [7] X. Gu, K. Huang, J. Zhang, and L. Huang, “Fast federated learning in the presence of arbitrary device unavailability,” *Advances in Neural Information Processing Systems*, vol. 34, pp. 12 052–12 064, 2021.
- [8] S. Wang and M. Ji, “A unified analysis of federated learning with arbitrary client participation,” in *Advances in Neural Information Processing Systems*, A. H. Oh, A. Agarwal, D. Belgrave, and K. Cho, Eds., 2022. [Online]. Available: <https://openreview.net/forum?id=qSs7C7c4G8D>
- [9] Y. Yan, C. Niu, Y. Ding, Z. Zheng, S. Tang, Q. Li, F. Wu, C. Lyu, Y. Feng, and G. Chen, “Federated optimization under intermittent client availability,” *INFORMS Journal on Computing*, 2023.
- [10] H. Yang, X. Zhang, P. Khanduri, and J. Liu, “Anarchic federated learning,” in *International Conference on Machine Learning*. PMLR, 2022, pp. 25 331–25 363.
- [11] N. A. Lynch, *Distributed algorithms*. Elsevier, 1996.
- [12] S. Bonomi, A. Del Pozzo, M. Potop-Butucaru, and S. Tixeuil, “Approximate agreement under mobile byzantine faults,” *Theoretical Computer Science*, vol. 758, pp. 17–29, 2019.

- [13] S. Ghadimi and G. Lan, “Stochastic first-and zeroth-order methods for nonconvex stochastic programming,” *SIAM Journal on Optimization*, vol. 23, no. 4, pp. 2341–2368, 2013.
- [14] A. Nemirovski, A. Juditsky, G. Lan, and A. Shapiro, “Robust stochastic approximation approach to stochastic programming,” *SIAM Journal on optimization*, vol. 19, no. 4, pp. 1574–1609, 2009.
- [15] Y. Arjevani, Y. Carmon, J. C. Duchi, D. J. Foster, N. Srebro, and B. Woodworth, “Lower bounds for non-convex stochastic optimization,” *Mathematical Programming*, pp. 1–50, 2022.
- [16] X. Yuan and P. Li, “On convergence of fedprox: Local dissimilarity invariant bounds, non-smoothness and beyond,” in *Advances in Neural Information Processing Systems*, A. H. Oh, A. Agarwal, D. Belgrave, and K. Cho, Eds., 2022. [Online]. Available: https://openreview.net/forum?id=_33ynl9VgCX
- [17] J. Chen and S. Micali, “Algorand,” *arXiv preprint arXiv:1607.01341*, 2016.
- [18] J. Feng, H. Xu, and S. Mannor, “Distributed robust learning,” *arXiv preprint arXiv:1409.5937*, 2014.
- [19] S. Sundaram and B. Ghahsifard, “Consensus-based distributed optimization with malicious nodes,” in *2015 53rd Annual Allerton Conference on Communication, Control, and Computing (Allerton)*. IEEE, 2015, pp. 244–249.
- [20] L. Su and N. H. Vaidya, “Fault-tolerant multi-agent optimization: optimal iterative distributed algorithms,” in *Proceedings of the 2016 ACM symposium on principles of distributed computing*, 2016, pp. 425–434.
- [21] P. Blanchard, E. M. El Mhamdi, R. Guerraoui, and J. Stainer, “Machine learning with adversaries: Byzantine tolerant gradient descent,” *Advances in Neural Information Processing Systems*, vol. 30, 2017.
- [22] Y. Chen, L. Su, and J. Xu, “Distributed statistical machine learning in adversarial settings: Byzantine gradient descent,” *Proceedings of the ACM on Measurement and Analysis of Computing Systems*, vol. 1, no. 2, pp. 1–25, 2017.
- [23] D. Yin, Y. Chen, R. Kannan, and P. Bartlett, “Byzantine-robust distributed learning: Towards optimal statistical rates,” in *International Conference on Machine Learning*, 2018, pp. 5650–5659.
- [24] C. Xie, S. Koyejo, and I. Gupta, “Zeno: Distributed stochastic gradient descent with suspicion-based fault-tolerance,” in *International Conference on Machine Learning*, 2019, pp. 6893–6901.
- [25] A. Ghosh, R. K. Maity, S. Kadhe, A. Mazumdar, and K. Ramachandran, “Communication efficient and byzantine tolerant distributed learning,” in *2020 IEEE International Symposium on Information Theory (ISIT)*. IEEE, 2020, pp. 2545–2550.
- [26] S. P. Karimireddy, L. He, and M. Jaggi, “Learning from history for byzantine robust optimization,” in *International Conference on Machine Learning*. PMLR, 2021, pp. 5311–5319.
- [27] —, “Byzantine-robust learning on heterogeneous datasets via bucketing,” in *International Conference on Learning Representations*. PMLR, 2022.

- [28] S. Farhadkhani, R. Guerraoui, N. Gupta, R. Pinot, and J. Stephan, “Byzantine machine learning made easy by resilient averaging of momentums,” in *International Conference on Machine Learning*. PMLR, 2022, pp. 6246–6283.
- [29] Y. Allouah, S. Farhadkhani, R. Guerraoui, N. Gupta, R. Pinot, and J. Stephan, “Fixing by mixing: A recipe for optimal byzantine ml under heterogeneity,” in *Proceedings of The 26th International Conference on Artificial Intelligence and Statistics*, vol. 206. PMLR, 25–27 Apr 2023, pp. 1232–1300.
- [30] L. Su and J. Xu, “Securing distributed gradient descent in high dimensional statistical learning,” *Proceedings of the ACM on Measurement and Analysis of Computing Systems*, vol. 3, no. 1, pp. 1–41, 2019.
- [31] T. Li, A. K. Sahu, M. Zaheer, M. Sanjabi, A. Talwalkar, and V. Smith, “Federated optimization in heterogeneous networks,” *Proceedings of Machine Learning and Systems*, vol. 2, pp. 429–450, 2020.
- [32] S. P. Karimireddy, S. Kale, M. Mohri, S. Reddi, S. Stich, and A. T. Suresh, “Scaffold: Stochastic controlled averaging for federated learning,” in *International Conference on Machine Learning*. PMLR, 2020, pp. 5132–5143.
- [33] D. Jhunjunwala, P. Sharma, A. Nagarkatti, and G. Joshi, “Fedvarp: Tackling the variance due to partial client participation in federated learning,” in *Uncertainty in Artificial Intelligence*. PMLR, 2022, pp. 906–916.
- [34] J. Wang, Q. Liu, H. Liang, G. Joshi, and H. V. Poor, “Tackling the objective inconsistency problem in heterogeneous federated optimization,” *Advances in neural information processing systems*, vol. 33, pp. 7611–7623, 2020.
- [35] A. Krizhevsky, G. Hinton *et al.*, “Learning multiple layers of features from tiny images,” 2009.
- [36] O. Shamir, N. Srebro, and T. Zhang, “Communication-efficient distributed optimization using an approximate newton-type method,” in *International conference on machine learning*. PMLR, 2014, pp. 1000–1008.
- [37] K. Pillutla, S. M. Kakade, and Z. Harchaoui, “Robust aggregation for federated learning,” *IEEE Transactions on Signal Processing*, vol. 70, pp. 1142–1154, 2022.
- [38] H. Hsu, H. Qi, and M. Brown, “Measuring the effects of non-identical data distribution for federated visual classification,” 2019. [Online]. Available: <https://arxiv.org/abs/1909.06335>
- [39] H. Wang, M. Yurochkin, Y. Sun, D. Papailiopoulos, and Y. Khazaeni, “Federated learning with matched averaging,” in *International Conference on Learning Representations*, 2020. [Online]. Available: <https://openreview.net/forum?id=BkluqlSFDS>
- [40] Y. LeCun, L. Bottou, Y. Bengio, and P. Haffner, “Gradient-based learning applied to document recognition,” *Proceedings of the IEEE*, vol. 86, no. 11, pp. 2278–2324, 1998.
- [41] S. Caldas, S. M. K. Duddu, P. Wu, T. Li, J. Konečný, H. B. McMahan, V. Smith, and A. Talwalkar, “Leaf: A benchmark for federated settings,” *arXiv preprint arXiv:1812.01097*, 2018.

- [42] A. Paszke, S. Gross, F. Massa, A. Lerer, J. Bradbury, G. Chanan, T. Killeen, Z. Lin, N. Gimelshein, L. Antiga *et al.*, “Pytorch: An imperative style, high-performance deep learning library,” *Advances in neural information processing systems*, vol. 32, 2019.

Appendices

A Characterization of convergence speed in the non-convex case

In Corollary 4.4, the $\tilde{O}(1/\sqrt{T})$ convergence rate matches that of the standard stochastic gradient descent for optimizing nonconvex functions [13]. In fact, the $O(1/\sqrt{T})$ convergence rate is the best possible for any first-order method that has only access to noisy gradients (see e.g. [15, Theorem 3]). When there is no adversarial dropout, our results in Corollary 4.4 are comparable to the state-of-the-art convergence results for FedAvg or FedProx. Specifically, For FedAvg, decay terms similar to $\Delta B^2/T$ and $(G + \sigma)/\sqrt{T}$ also appear in [32, Theorem V]. For FedProx, [16, Theorem 1] assumes $B = 0$ and obtains a decay term similar to $(\Delta + G^2)/\sqrt{T}$.

Proof of Corollary 4.4. In the first case, $\eta_t = \eta_0$ is a constant for a given T . We obtain from Theorem 4.3 that

$$\mathbb{E}\|\nabla F(\theta_R)\|_2^2 \leq \frac{3\Delta}{\beta p s T \eta_0} + (4\epsilon + c\beta s L \eta_0)(G + \sigma)^2.$$

Plugging $\eta_0 \leq \frac{1}{\beta\sqrt{pTL}(G+\sigma)}$ and $\frac{1}{\eta_0} \leq 10\beta LB^2 + \beta\sqrt{pTL}(G + \sigma)$ yields that

$$\mathbb{E}\|\nabla F(\theta_R)\|_2^2 \leq \frac{30\Delta LB^2}{psT} + \sqrt{\frac{L}{pT}}(3\Delta/s + cs)(G + \sigma) + 4\epsilon(G + \sigma)^2.$$

In the second case where $\eta_t = \eta_0/\sqrt{t+1}$, it follows from Theorem 4.3 that

$$\mathbb{E}\|\nabla F(\theta_R)\|_2^2 \leq \frac{3\Delta}{\beta p s \eta_0 \sum_{t=0}^T \frac{1}{\sqrt{t+1}}} + \left(4\epsilon + c\beta s L \eta_0 \frac{\sum_{t=0}^T \frac{1}{t+1}}{\sum_{t=0}^T \frac{1}{\sqrt{t+1}}}\right)(G + \sigma)^2.$$

Note that $\sum_{t=0}^T \frac{1}{\sqrt{t+1}} \geq \int_1^{T+2} \frac{1}{\sqrt{x}} dx = 2\sqrt{T+2} - 2 \geq \sqrt{T}$ and $\sum_{t=0}^T \frac{1}{t+1} \leq 1 + \int_1^{T+1} \frac{1}{x} dx = \log(e(T+1))$. Plugging $\eta_0 \leq \frac{1}{\beta\sqrt{pL}(G+\sigma)}$ and $\frac{1}{\eta_0} \leq 10\beta LB^2 + \beta\sqrt{pL}(G + \sigma)$ yields that

$$\mathbb{E}\|\nabla F(\theta_R)\|_2^2 \leq \frac{30\Delta LB^2}{ps\sqrt{T}} + \sqrt{\frac{L}{pT}}(3\Delta/s + cs \log(e(T+1)))(G + \sigma) + 4\epsilon(G + \sigma)^2.$$

□

B Proofs of upper bounds

B.1 Proof of Theorem 4.3

We first prove the results for the FedAvg update rule.

B.1.1 Proofs of auxiliary lemmas

Proof of Lemma 5.1 . By the definition of κ ,

$$\kappa \eta_t^2 \binom{s}{2} L_i \geq \frac{(1 + \eta_t L_i)^s - 1 - s \eta_t L_i}{L_i}.$$

Hence it suffices to show

$$\|\theta - \mathcal{G}_{i,t}^s(\theta; \eta_t) - s\eta_t \nabla \ell_{i,t}(\theta)\|_2 \leq \frac{(1 + \eta_t L_i)^s - 1 - s\eta_t L_i}{(\eta_t L_i)^2} \eta_t^2 L_i \|\nabla \ell_{i,t}(\theta)\|_2. \quad (24)$$

We prove (24) holds for all $s \geq 1$ by induction. The base case $s = 1$ follows from the definition of gradient mapping $\mathcal{G}_{i,t}$ in (13). Suppose (24) holds true for $s = 1, \dots, n-1$, where $n \geq 2$. Next we prove (24) for $s = n$. By the telescoping sum

$$\mathcal{G}_{i,t}^n(\theta; \eta_t) - \theta = \sum_{s=0}^{n-1} \mathcal{G}_{i,t}^{s+1}(\theta; \eta_t) - \mathcal{G}_{i,t}^s(\theta; \eta_t) = -\eta_t \sum_{s=0}^{n-1} \nabla \ell_{i,t}(\mathcal{G}_{i,t}^s(\theta; \eta_t)),$$

we obtain

$$\begin{aligned} \|\theta - \mathcal{G}_{i,t}^n(\theta; \eta_t) - n\eta_t \nabla \ell_{i,t}(\theta)\|_2 &= \eta_t \left\| \sum_{s=0}^{n-1} (\nabla \ell_{i,t}(\mathcal{G}_{i,t}^s(\theta; \eta_t)) - \nabla \ell_{i,t}(\theta)) \right\|_2 \leq \eta_t L_i \sum_{s=0}^{n-1} \|\mathcal{G}_{i,t}^s(\theta; \eta_t) - \theta\|_2 \\ &\leq \eta_t L_i \sum_{s=1}^{n-1} \left(\|\theta - \mathcal{G}_{i,t}^s(\theta; \eta_t) - s\eta_t \nabla \ell_{i,t}(\theta)\|_2 + s\eta_t \|\nabla \ell_{i,t}(\theta)\|_2 \right), \end{aligned} \quad (25)$$

where in the first inequality we used (4). Applying the induction hypothesis (24) for $s = 1, \dots, n-1$, we get

$$\sum_{s=1}^{n-1} \|\theta - \mathcal{G}_{i,t}^s(\theta; \eta_t) - s\eta_t \nabla \ell_{i,t}(\theta)\|_2 \leq \left((1 + \eta_t L_i)^n - 1 - n\eta_t L_i - \binom{n}{2} (\eta_t L_i)^2 \right) \frac{\|\nabla \ell_{i,t}(\theta)\|_2}{\eta_t L_i^2}.$$

Plugging into (25), we conclude (24) for $s = n$. The proof is completed. \square

Proof of Lemma 5.2. For any $t \geq 1$, it holds that

$$\begin{aligned} \left\| \sum_{i \in \tilde{\mathcal{S}}_t \setminus \mathcal{S}_t} w_i \nabla \ell_{i,t}(\theta_t) \right\|_2^2 &= \sum_{i,j \in \tilde{\mathcal{S}}_t \setminus \mathcal{S}_t} w_i w_j \langle \nabla \ell_{i,t}(\theta_t), \nabla \ell_{j,t}(\theta_t) \rangle \\ &\stackrel{(a)}{\leq} \sum_{i,j \in \tilde{\mathcal{S}}_t \setminus \mathcal{S}_t} w_i w_j \frac{\|\nabla \ell_{i,t}(\theta_t)\|_2^2 + \|\nabla \ell_{j,t}(\theta_t)\|_2^2}{2} \\ &= \left(\sum_{i \in \tilde{\mathcal{S}}_t \setminus \mathcal{S}_t} w_i \right) \left(\sum_{i \in \tilde{\mathcal{S}}_t \setminus \mathcal{S}_t} w_i \|\nabla \ell_{i,t}(\theta_t)\|_2^2 \right) \\ &\leq \left(\sum_{i \in \tilde{\mathcal{S}}_t \setminus \mathcal{S}_t} w_i \right) \left(\sum_{i \in \tilde{\mathcal{S}}_t} w_i \|\nabla \ell_{i,t}(\theta_t)\|_2^2 \right). \end{aligned} \quad (26)$$

where inequality (a) follows from the fact that $\langle u, v \rangle \leq \frac{1}{2}(\|u\|_2^2 + \|v\|_2^2)$ for any u, v of the same dimension. Notably, Eq.(26) is the key step that enables us to control $\mathbb{E} \left[\left\| \sum_{i \in \tilde{\mathcal{S}}_t \setminus \mathcal{S}_t} w_i \nabla \ell_{i,t}(\theta_t) \right\|_2^2 \mid \mathcal{F}_t \right]$ in terms of ϵ . By Assumption 3.2, we have

$$\sum_{i \in \tilde{\mathcal{S}}_t \setminus \mathcal{S}_t} w_i = \sum_{i \in \tilde{\mathcal{S}}_t \setminus \mathcal{S}_t} \frac{n_i}{N} \leq \frac{K\epsilon}{M} = p\epsilon. \quad (27)$$

Hence, it suffices to show

$$\mathbb{E} \left[\sum_{i \in \tilde{\mathcal{S}}_t} w_i \|\nabla \ell_{i,t}(\theta_t)\|_2^2 \mid \mathcal{F}_t \right] \leq p \left(B^2 \|\nabla F(\theta_t)\|_2^2 + G^2 + \sigma^2 \right),$$

for which we have

$$\begin{aligned} \mathbb{E} \left[\sum_{i \in \tilde{\mathcal{S}}_t} w_i \|\nabla \ell_{i,t}(\theta_t)\|_2^2 \mid \mathcal{F}_t \right] &= \mathbb{E} \left[\sum_{i=1}^M w_i \|\nabla \ell_{i,t}(\theta_t)\|_2^2 \mathbf{1}_{\{i \in \tilde{\mathcal{S}}_t\}} \mid \mathcal{F}_t \right] \\ &\stackrel{(a)}{=} \sum_{i=1}^M w_i \mathbb{E} \left[\|\nabla \ell_{i,t}(\theta_t)\|_2^2 \mid \mathcal{F}_t \right] \mathbb{E} \left[\mathbf{1}_{\{i \in \tilde{\mathcal{S}}_t\}} \mid \mathcal{F}_t \right] \\ &\stackrel{(b)}{=} p \sum_{i=1}^M w_i \mathbb{E} \left[\|\nabla \ell_{i,t}(\theta_t)\|_2^2 \mid \mathcal{F}_t \right] \\ &\stackrel{(c)}{\leq} p \sum_{i \in [M]} w_i \left(\|\nabla F_i(\theta_t)\|_2^2 + \sigma_i^2 \right) \\ &\stackrel{(d)}{=} p \left(\sum_{i \in [M]} w_i \|\nabla F_i(\theta_t)\|_2^2 + \sigma^2 \right) \\ &\stackrel{(e)}{\leq} p \left(B^2 \|\nabla F(\theta_t)\|_2^2 + G^2 + \sigma^2 \right), \end{aligned} \tag{28}$$

where equality (a) is true because, as mentioned before, $\tilde{\mathcal{S}}_t$ and $z_{i,t}$ are mutually independent; equality (b) holds because $\tilde{\mathcal{S}}_t$ is independent of \mathcal{F}_t ; inequality (c) follows from the fact that θ_t is adapted to \mathcal{F}_t and (7), so that

$$\mathbb{E} \left[\|\nabla \ell_{i,t}(\theta_t)\|_2^2 \mid \mathcal{F}_t \right] = \|\nabla F_i(\theta_t)\|_2^2 + \mathbb{E} \left[\|\nabla \ell_{i,t}(\theta_t) - \nabla F_i(\theta_t)\|_2^2 \mid \mathcal{F}_t \right] \leq \|\nabla F_i(\theta_t)\|_2^2 + \sigma_i^2;$$

equality (d) uses the definition of σ^2 ; and inequality (e) follows from Assumption 3.1. The conclusion follows from (26), (27), and (28). \square

B.1.2 Bound on the decrease of the objective function

We are ready to analyze the decrease of the objective function values specified on the right-hand side of (11) under our dropout model.

It follows from our aggregation rule (3) that, for every t ,

$$\begin{aligned} \theta_{t+1} - \theta_t &= \beta \sum_{i \in \mathcal{S}_t} w_i (\mathcal{G}_{i,t}^s(\theta_t; \eta_t) - \theta_t) \\ &= \beta \sum_{i \in \mathcal{S}_t} w_i (\mathcal{G}_{i,t}^s(\theta_t; \eta_t) - \theta_t + s \eta_t \nabla \ell_{i,t}(\theta_t)) - \beta s \eta_t \sum_{i \in \mathcal{S}_t} w_i \nabla \ell_{i,t}(\theta_t). \end{aligned} \tag{29}$$

Bounding $\mathbb{E}[\langle \nabla F(\theta_t), \theta_{t+1} - \theta_t \rangle \mid \mathcal{F}_t]$: Plugging (29), the second term on the right-hand side of (11) is decomposed into

$$\begin{aligned} \langle \nabla F(\theta_t), \theta_{t+1} - \theta_t \rangle &= \beta \cdot \underbrace{\left\langle \nabla F(\theta_t), \sum_{i \in \mathcal{S}_t} w_i (\mathcal{G}_{i,t}^s(\theta_t; \eta_t) - \theta_t + s\eta_t \nabla \ell_{i,t}(\theta_t)) \right\rangle}_{\text{(I)}} \\ &\quad - \beta s \eta_t \cdot \underbrace{\left\langle \nabla F(\theta_t), \sum_{i \in \mathcal{S}_t} w_i \nabla \ell_{i,t}(\theta_t) \right\rangle}_{\text{(II)}}. \end{aligned} \quad (30)$$

On (I), we have

$$\text{(I)} \leq \|\nabla F(\theta_t)\|_2 \left\| \sum_{i \in \mathcal{S}_t} w_i (\mathcal{G}_{i,t}^s(\theta_t; \eta_t) - \theta_t + s\eta_t \nabla \ell_{i,t}(\theta_t)) \right\|_2$$

and hence

$$\mathbb{E}[\text{(I)} \mid \mathcal{F}_t] \leq p \|\nabla F(\theta_t)\|_2 \kappa \eta_t^2 L \binom{s}{2} (B \|\nabla F(\theta_t)\|_2 + G + \sigma), \quad (31)$$

where the last inequality holds by (18).

For the lower bound of (II), we consider the difference of clients belonging to \mathcal{S}_t and $\tilde{\mathcal{S}}_t$:

$$\begin{aligned} \text{(II)} &= \left\langle \nabla F(\theta_t), \sum_{i \in \tilde{\mathcal{S}}_t} w_i \nabla \ell_{i,t}(\theta_t) \right\rangle - \left\langle \nabla F(\theta_t), \sum_{i \in \tilde{\mathcal{S}}_t \setminus \mathcal{S}_t} w_i \nabla \ell_{i,t}(\theta_t) \right\rangle \\ &\geq \left\langle \nabla F(\theta_t), \sum_{i \in \tilde{\mathcal{S}}_t} w_i \nabla \ell_{i,t}(\theta_t) \right\rangle - \|\nabla F(\theta_t)\|_2 \left\| \sum_{i \in \tilde{\mathcal{S}}_t \setminus \mathcal{S}_t} w_i \nabla \ell_{i,t}(\theta_t) \right\|_2. \end{aligned}$$

Thus,

$$\begin{aligned} \mathbb{E}[\text{(II)} \mid \mathcal{F}_t] &\geq \mathbb{E} \left[\left\langle \nabla F(\theta_t), \sum_{i \in \tilde{\mathcal{S}}_t} w_i \nabla \ell_{i,t}(\theta_t) \right\rangle - \|\nabla F(\theta_t)\|_2 \left\| \sum_{i \in \tilde{\mathcal{S}}_t \setminus \mathcal{S}_t} w_i \nabla \ell_{i,t}(\theta_t) \right\|_2 \mid \mathcal{F}_t \right] \\ &= \left\langle \nabla F(\theta_t), \mathbb{E} \left[\sum_{i \in \tilde{\mathcal{S}}_t} w_i \nabla \ell_{i,t}(\theta_t) \mid \mathcal{F}_t \right] \right\rangle - \|\nabla F(\theta_t)\|_2 \mathbb{E} \left[\left\| \sum_{i \in \tilde{\mathcal{S}}_t \setminus \mathcal{S}_t} w_i \nabla \ell_{i,t}(\theta_t) \right\|_2 \mid \mathcal{F}_t \right] \\ &\stackrel{(a)}{\geq} p \|\nabla F(\theta_t)\|_2^2 - p \|\nabla F(\theta_t)\|_2 \sqrt{\epsilon} (B \|\nabla F(\theta_t)\|_2 + G + \sigma), \end{aligned} \quad (32)$$

where equality (a) follows from (20) and Lemma 5.2.

Combining (32) and (31) together and plugging it back to (30), we get that

$$\begin{aligned} \mathbb{E}[\langle \nabla F(\theta_t), \theta_{t+1} - \theta_t \rangle \mid \mathcal{F}_t] &\leq -\beta p s \eta_t \|\nabla F(\theta_t)\|_2^2 + \beta p s \eta_t \|\nabla F(\theta_t)\|_2 \sqrt{\epsilon} (B \|\nabla F(\theta_t)\|_2 + G + \sigma) \\ &\quad + \beta p \|\nabla F(\theta_t)\|_2 \kappa \eta_t^2 L \binom{s}{2} (B \|\nabla F(\theta_t)\|_2 + G + \sigma). \end{aligned} \quad (33)$$

Bounding $\mathbb{E} [\|\theta_{t+1} - \theta_t\|_2^2 \mid \mathcal{F}_t]$: By (29), we have

$$\begin{aligned}
\|\theta_{t+1} - \theta_t\|_2 &= \left\| \beta \sum_{i \in \mathcal{S}_t} w_i (\mathcal{G}_{i,t}^s(\theta_t; \eta_t) - \theta_t + s\eta_t \nabla \ell_{i,t}(\theta_t)) - \beta s\eta_t \sum_{i \in \mathcal{S}_t} w_i \nabla \ell_{i,t}(\theta_t) \right\|_2 \\
&\stackrel{(a)}{\leq} \beta s\eta_t \left\| \sum_{i \in \mathcal{S}_t} w_i \nabla \ell_{i,t}(\theta_t) \right\|_2 + \beta \kappa \eta_t^2 L \binom{s}{2} \sum_{i \in \mathcal{S}_t} w_i \|\nabla \ell_{i,t}(\theta_t)\|_2 \\
&\leq \beta s\eta_t (1 + \kappa \eta_t L(s-1)/2) \sum_{i \in \mathcal{S}_t} w_i \|\nabla \ell_{i,t}(\theta_t)\|_2 \\
&\leq \beta s\eta_t (1 + \kappa \eta_t L(s-1)/2) \sqrt{\sum_{i \in \tilde{\mathcal{S}}_t} w_i} \sqrt{\sum_{i \in \tilde{\mathcal{S}}_t} w_i \|\nabla \ell_{i,t}(\theta_t)\|_2^2}.
\end{aligned}$$

where inequality (a) follows from Lemma 5.1 and the fact that $L = \max_{i \in [M]} L_i$; the last inequality holds by the Cauchy-Schwarz inequality. Applying (28) and using $\sum_{i \in \tilde{\mathcal{S}}_t} w_i \leq 1$, we deduce that

$$\mathbb{E} [\|\theta_{t+1} - \theta_t\|_2^2 \mid \mathcal{F}_t] \leq \beta^2 s^2 \eta_t^2 (1 + \kappa \eta_t L(s-1)/2)^2 p \left(B^2 \|\nabla F(\theta)\|_2^2 + G^2 + \sigma^2 \right). \quad (34)$$

Bounding $\mathbb{E} [F(\theta_{t+1}) \mid \mathcal{F}_t]$: Combining (33) and (34) together, we apply (11) and get

$$\mathbb{E} [F(\theta_{t+1}) \mid \mathcal{F}_t] \leq F(\theta_t) - \bar{a}_t \|\nabla F(\theta_t)\|_2^2 + b_t \|\nabla F(\theta_t)\|_2 + c_t,$$

where

$$\begin{aligned}
\bar{a}_t &= \beta p s \eta_t \left(1 - \sqrt{\epsilon} B - \frac{\kappa(s-1)\eta_t L}{2} B - \beta \frac{s\eta_t L}{2} \left(1 + \frac{\kappa(s-1)\eta_t L}{2} \right)^2 B^2 \right), \\
b_t &= \beta p s \eta_t \left(\sqrt{\epsilon} (G + \sigma) + \frac{\kappa(s-1)\eta_t L}{2} (G + \sigma) \right), \\
c_t &= \beta^2 p s \eta_t \frac{s\eta_t L}{2} \left(1 + \frac{\kappa(s-1)\eta_t L}{2} \right)^2 (G^2 + \sigma^2).
\end{aligned}$$

By the conditions on η_t and ϵ , we have $\sqrt{\epsilon} B < c_0 = 0.1$ and $\eta_t s L \leq \eta_t s L \beta B^2 \leq 0.1$, and thus $\kappa \leq \frac{e^{0.1}-1-0.1}{(0.1)^2/2} \leq 1.0342$. Then we get

$$\bar{a}_t \geq C_0 \cdot \beta p s \eta_t \triangleq a_t,$$

where $C_0 \geq 1 - c_0 - 0.05\kappa - 0.05(1 + 0.05\kappa)^2 \geq 0.7929 > 0$ is a constant. Hence,

$$\mathbb{E} [F(\theta_{t+1}) \mid \mathcal{F}_t] \leq F(\theta_t) - a_t \|\nabla F(\theta_t)\|_2^2 + b_t \|\nabla F(\theta_t)\|_2 + c_t,$$

Finishing the proof for FedAvg: Note that

$$\|\nabla F(\theta_t)\|_2 \leq a \|\nabla F(\theta_t)\|_2^2 + \frac{1}{4a}, \quad \forall a \geq 0.$$

Picking $a = \frac{a_t}{2b_t}$, we get

$$\mathbb{E} [F(\theta_{t+1})] \leq \mathbb{E} [F(\theta_t)] - \frac{a_t}{2} \mathbb{E} \|\nabla F(\theta_t)\|_2^2 + \frac{b_t^2}{2a_t} + c_t.$$

By telescoping sum, we get

$$\mathbb{E}[F(\theta_{T+1})] \leq F(\theta_0) - \frac{1}{2} \sum_{t=0}^T a_t \mathbb{E} \|\nabla F(\theta_t)\|_2^2 + \sum_{t=0}^T \left(\frac{b_t^2}{2a_t} + c_t \right).$$

Rearranging the terms, we deduce that

$$\frac{\sum_{t=0}^T \eta_t \mathbb{E} \|\nabla F(\theta_t)\|_2^2}{\sum_{t=0}^T \eta_t} = \frac{\sum_{t=0}^T a_t \mathbb{E} \|\nabla F(\theta_t)\|_2^2}{\sum_{t=0}^T a_t} \leq \frac{2(F(\theta_0) - F_{\min})}{\sum_{t=0}^T a_t} + \frac{\sum_{t=0}^T \left(\frac{b_t^2}{a_t} + 2c_t \right)}{\sum_{t=0}^T a_t}. \quad (35)$$

Since $a_t = C_0 \beta p s \eta_t$, we have

$$\begin{aligned} \frac{b_t^2}{a_t} + 2c_t &\leq \frac{\beta}{C_0} (ps\eta_t) 2(\epsilon + (C_1 s \eta_t L)^2) (G + \sigma)^2 + \beta^2 (ps\eta_t) (C_2 s \eta_t L) (G + \sigma)^2 \\ &\leq \frac{2\epsilon}{C_0} (G + \sigma)^2 \beta p s \eta_t + C_3 \beta^2 p s^2 \eta_t^2 L (G + \sigma)^2. \end{aligned}$$

where $C_1 = \frac{\kappa}{2}$, $C_2 = (1 + \frac{0.1\kappa}{2})^2$, and $C_3 = C_2 + \frac{0.2C_1^2}{C_0\beta}$. Hence,

$$\frac{\sum_{t=0}^T \left(\frac{b_t^2}{a_t} + 2c_t \right)}{\sum_{t=0}^T a_t} \leq \left(\frac{2\epsilon}{C_0^2} + \beta \frac{C' s L \sum_{t=0}^T \eta_t^2}{\sum_{t=0}^T \eta_t} \right) (G + \sigma)^2$$

for some universal constant C' , where $2/C_0^2 \leq 2/0.7929^2 < 3.2$. Plugging the last displayed equation back to (35) completes the proof of Theorem 4.3 for FedAvg.

B.1.3 Proof for FedProx

For FedProx, let $\mathcal{P}_{i,t}(\theta, \eta)$ denote proximal mapping defined as

$$\mathcal{P}_{i,t}(\theta; \eta) \triangleq \arg \min_z \ell_{i,t}(z) + \frac{1}{2\eta} \|z - \theta\|_2^2. \quad (36)$$

Then $\theta_{i,t+1} \in \mathcal{P}_{i,t}(\theta_t; \eta_t)$.

The proof for the FedProx is similar, where we need an analogous result to Lemma 5.1 under the additional condition that $\lambda_{\min}(\nabla^2 \ell_{i,t}(\theta)) \geq -L_-$ for all i . This condition is standard in analyzing the FedProx algorithm [3]. Note that the following result and proof can be readily extended to the case where the proximal problem (36) at each local step is solved inexactly (see e.g. [16, Lemma 5]).

Lemma B.1. *Suppose $\lambda_{\min}(\nabla^2 \ell_{i,t}(\theta)) \geq -L_-$. Then for $\eta < \frac{1}{L_-}$, we have*

$$\|\theta - \mathcal{P}_{i,t}(\theta; \eta) - \eta \nabla \ell_{i,t}(\theta)\|_2 \leq \frac{\eta^2}{1 - \eta L_-} L_i \|\nabla \ell_{i,t}(\theta)\|_2, \quad \forall \theta.$$

Proof. For $\eta < \frac{1}{L_-}$, the local objective function $\tilde{\ell}_{i,t}(z) \triangleq \ell_{i,t}(z) + \frac{1}{2\eta} \|z - \theta\|_2^2$ as given in (36) is $(1/\eta - L_-)$ -strongly convex in view of the definition (10). Hence, the optimization program (36) has a unique minimizer. By the first-order optimality condition,

$$\theta - \mathcal{P}_{i,t}(\theta, \eta) = \eta \nabla \ell_{i,t}(\mathcal{P}_{i,t}(\theta, \eta)).$$

By the $(\frac{1}{\eta} - L_-)$ -strong convexity of the objective function $\tilde{\ell}_{i,t}(z)$, we have

$$\|\mathcal{P}_{i,t}(\theta, \eta) - \theta\|_2 \leq \frac{1}{\frac{1}{\eta} - L_-} \left\| \nabla \tilde{\ell}_{i,t}(\mathcal{P}_{i,t}(\theta, \eta)) - \nabla \tilde{\ell}_{i,t}(\theta) \right\|_2 = \frac{1}{\frac{1}{\eta} - L_-} \|\nabla \ell_{i,t}(\theta)\|_2,$$

where we used the facts that $\nabla \tilde{\ell}_{i,t}(\mathcal{P}_{i,t}(\theta, \eta)) = 0$ and $\nabla \tilde{\ell}_{i,t}(\theta) = \nabla \ell_{i,t}(\theta)$. Therefore, by the smoothness of $\ell_{i,t}$, we have

$$\begin{aligned} \|\theta - \mathcal{P}_{i,t}(\theta, \eta) - \eta \nabla \ell_{i,t}(\theta)\|_2 &= \eta \|\nabla \ell_{i,t}(\mathcal{P}_{i,t}(\theta, \eta)) - \nabla \ell_{i,t}(\theta)\|_2 \leq \eta L_i \|\mathcal{P}_{i,t}(\theta, \eta) - \theta\|_2 \\ &\leq \frac{\eta^2 L_i}{1 - \eta L_-} \|\nabla \ell_{i,t}(\theta)\|_2. \end{aligned} \quad \square$$

The remaining analysis is similar to the FedAvg update rule. In particular, following the previous arguments, we upper bound the right-hand side of (11) by

$$\begin{aligned} \mathbb{E}[\langle \nabla F(\theta_t), \theta_{t+1} - \theta_t \rangle \mid \mathcal{F}_t] &\leq -\beta p \eta_t \|\nabla F(\theta_t)\|_2^2 + \beta p \eta_t \|\nabla F(\theta_t)\|_2 \sqrt{\epsilon} (B \|\nabla F(\theta_t)\|_2 + G + \sigma) \\ &\quad + \beta p \|\nabla F(\theta_t)\|_2 \frac{\eta_t^2}{1 - \eta_t L_-} L (B \|\nabla F(\theta_t)\|_2 + G + \sigma), \end{aligned} \quad (37)$$

$$\mathbb{E}[\|\theta_{t+1} - \theta_t\|_2^2 \mid \mathcal{F}_t] \leq \beta^2 \eta_t^2 \left(1 + \frac{\eta_t L}{1 - \eta_t L_-}\right)^2 p (B^2 \|\nabla F(\theta_t)\|_2^2 + G^2 + \sigma^2). \quad (38)$$

Then, we get

$$\mathbb{E}[F(\theta_{t+1}) \mid \mathcal{F}_t] \leq F(\theta_t) - \bar{a}'_t \|\nabla F(\theta_t)\|_2^2 + b'_t \|\nabla F(\theta_t)\|_2 + c'_t,$$

where

$$\begin{aligned} \bar{a}'_t &= \beta p \eta_t \left(1 - \sqrt{\epsilon} B - \frac{\eta_t L}{1 - \eta_t L_-} B - \beta \frac{\eta_t L}{2} \left(1 + \frac{\eta_t L}{1 - \eta_t L_-}\right)^2 B^2\right), \\ b'_t &= \beta p \eta_t \left(\sqrt{\epsilon} (G + \sigma) + \frac{\eta_t L}{1 - \eta_t L_-} (G + \sigma)\right), \\ c'_t &= \beta^2 p \eta_t \frac{\eta_t L}{2} \left(1 + \frac{\eta_t L}{1 - \eta_t L_-}\right)^2 (G^2 + \sigma^2). \end{aligned}$$

By the conditions on η_t and ϵ , we have $\sqrt{\epsilon} B \leq c_0 = 0.1$, $\eta_t L \leq \eta_t \beta L B^2 \leq 0.1$, and $\eta_t L_- \leq 0.1$, and thus $\bar{a}'_t \geq C'_0 \cdot \beta p \eta_t \triangleq a'_t$, where $C'_0 \geq 1 - c_0 - 0.1/0.9 - 0.05 \times (1 + 0.1/0.9)^2 \geq 0.727$. Following a similar analysis, we get

$$\begin{aligned} \frac{\sum_{t=0}^T \eta_t \|\nabla F(\theta_t)\|_2^2}{\sum_{t=0}^T \eta_t} &= \frac{\sum_{t=0}^T a'_t \|\nabla F(\theta_t)\|_2^2}{\sum_{t=0}^T a'_t} \leq \frac{2(F(\theta_0) - F_{\min})}{\sum_{t=0}^T a'_t} + \frac{\sum_{t=0}^T \left(\frac{b_t'^2}{a_t'} + 2c_t'\right)}{\sum_{t=0}^T a'_t} \\ &\leq \frac{2(F(\theta_0) - F_{\min})}{\sum_{t=0}^T a'_t} + \left(\frac{2\epsilon}{C_0'^2} + \beta \frac{cL \sum_{t=0}^T \eta_t^2}{\sum_{t=0}^T \eta_t}\right) (G + \sigma)^2, \end{aligned}$$

where $2/C_0'^2 \leq 2/0.727^2 \leq 3.8$.

B.2 Proof of Theorem 4.5

Proof of Theorem 4.5. We first consider FedAvg. The proof is in the same spirit as that in the non-convex case. The major difference is that in the strongly convex setting, we study the iterates of $\Delta_t \triangleq \|\theta_t - \theta^*\|_2$, for which we have

$$\begin{aligned}\Delta_{t+1}^2 &= \|\theta_{t+1} - \theta_t + \theta_t - \theta^*\|_2^2 \\ &= \Delta_t^2 + 2\langle \theta_{t+1} - \theta_t, \theta_t - \theta^* \rangle + \|\theta_{t+1} - \theta_t\|_2^2.\end{aligned}\tag{39}$$

Let us first analyze the drift term $\langle \theta_{t+1} - \theta_t, \theta_t - \theta^* \rangle$. Plugging (29), we get that

$$\begin{aligned}\langle \theta_{t+1} - \theta_t, \theta_t - \theta^* \rangle &= \beta \underbrace{\left\langle \theta_t - \theta^*, \sum_{i \in \mathcal{S}_t} w_i (\mathcal{G}_{i,t}^s(\theta_t; \eta_t) - \theta_t + s\eta_t \nabla \ell_{i,t}(\theta_t)) \right\rangle}_{\text{(I)}} \\ &\quad - \beta s \eta_t \underbrace{\left\langle \theta_t - \theta^*, \sum_{i \in \mathcal{S}_t} w_i \nabla \ell_{i,t}(\theta_t) \right\rangle}_{\text{(II)}}.\end{aligned}$$

For term (I), analogous to (31), applying Lemma 5.1 and (17), we get

$$\begin{aligned}\mathbb{E}[(\text{I}) \mid \mathcal{F}_t] &\leq p \|\theta_t - \theta^*\|_2 \kappa \eta_t^2 L \binom{s}{2} (B \|\nabla F(\theta_t)\|_2 + G + \sigma) \\ &\leq p \|\theta_t - \theta^*\|_2 \kappa \eta_t^2 L \binom{s}{2} (BL \|\theta_t - \theta^*\|_2 + G + \sigma),\end{aligned}\tag{40}$$

where the last inequality follows from L -smoothness so that

$$\|\nabla F(\theta_t)\|_2 \leq L \|\theta_t - \theta^*\|_2$$

For term (II),

$$\begin{aligned}(\text{II}) &= \left\langle \theta_t - \theta^*, \sum_{i \in \tilde{\mathcal{S}}_t} w_i \nabla \ell_{i,t}(\theta_t) \right\rangle - \left\langle \theta_t - \theta^*, \sum_{i \in \tilde{\mathcal{S}}_t \setminus \mathcal{S}_t} w_i \nabla \ell_{i,t}(\theta_t) \right\rangle \\ &\geq \left\langle \theta_t - \theta^*, \sum_{i \in \tilde{\mathcal{S}}_t} w_i \nabla \ell_{i,t}(\theta_t) \right\rangle - \|\theta_t - \theta^*\|_2 \left\| \sum_{i \in \tilde{\mathcal{S}}_t \setminus \mathcal{S}_t} w_i \nabla \ell_{i,t}(\theta_t) \right\|_2\end{aligned}$$

Then, applying (20) and Lemma 5.2 yields

$$\mathbb{E}[(\text{II}) \mid \mathcal{F}_t] \geq p (\langle \theta_t - \theta^*, \nabla F(\theta_t) \rangle - \|\theta_t - \theta^*\|_2 \sqrt{\epsilon} (B \|\nabla F(\theta_t)\|_2 + G + \sigma)).\tag{41}$$

By μ -strong convexity, we have

$$\langle \theta_t - \theta^*, \nabla F(\theta_t) \rangle \geq \mu \|\theta_t - \theta^*\|_2^2.$$

By L -smoothness, we have

$$\|\nabla F(\theta_t)\|_2 \leq L \|\theta_t - \theta^*\|_2$$

It follows that

$$\mathbb{E}[(\text{II}) \mid \mathcal{F}_t] \geq p \left(\mu \|\theta_t - \theta^*\|_2^2 - \|\theta_t - \theta^*\|_2 \sqrt{\epsilon} (BL \|\theta_t - \theta^*\|_2 + G + \sigma) \right). \quad (42)$$

Combining the last displayed equation with (40) yields that

$$\begin{aligned} & \mathbb{E}[\langle \theta_{t+1} - \theta_t, \theta_t - \theta^* \rangle \mid \mathcal{F}_t] \\ & \leq -\beta p s \eta_t \mu \|\theta_t - \theta^*\|_2^2 + \beta p s \eta_t \|\theta_t - \theta^*\|_2 \sqrt{\epsilon} (BL \|\theta_t - \theta^*\|_2 + G + \sigma) \\ & \quad + \beta p \|\theta_t - \theta^*\|_2 \kappa \eta_t^2 L \binom{s}{2} (BL \|\theta_t - \theta^*\|_2 + G + \sigma). \end{aligned} \quad (43)$$

For the quadratic term, analogous to (34), we have

$$\begin{aligned} \mathbb{E}[\|\theta_{t+1} - \theta_t\|_2^2 \mid \mathcal{F}_t] & \leq \beta^2 s^2 \eta_t^2 (1 + \kappa \eta_t L(s-1)/2)^2 p \left(B^2 \|\nabla F(\theta)\|_2^2 + G^2 + \sigma^2 \right) \\ & \leq \beta^2 s^2 \eta_t^2 (1 + \kappa \eta_t L(s-1)/2)^2 p \left(B^2 L^2 \|\theta_t - \theta^*\|_2^2 + G^2 + \sigma^2 \right). \end{aligned}$$

Combining the last two displayed equations and plugging them into (39) yields that

$$\begin{aligned} \mathbb{E}[\Delta_{t+1}^2 \mid \mathcal{F}_t] & \leq \Delta_t^2 - 2\beta p s \eta_t \mu \Delta_t^2 + 2\beta p s \eta_t \Delta_t \sqrt{\epsilon} (BL \Delta_t + G + \sigma) \\ & \quad + 2\beta p \Delta_t \kappa \eta_t^2 L \binom{s}{2} (BL \Delta_t + G + \sigma) \\ & \quad + \beta^2 s^2 \eta_t^2 (1 + \kappa \eta_t L(s-1)/2)^2 p (B^2 L^2 \Delta_t^2 + G^2 + \sigma^2). \end{aligned}$$

In particular,

$$\mathbb{E}[\Delta_{t+1}^2 \mid \mathcal{F}_t] \leq (1 - a_t) \Delta_t^2 + b_t \Delta_t + c_t,$$

where

$$\begin{aligned} a_t & = 2\beta p s \eta_t \left(\mu - \sqrt{\epsilon} BL - \eta_t \kappa \frac{s-1}{2} BL^2 - \frac{1}{2} \beta s \eta_t (1 + \kappa \eta_t L(s-1)/2)^2 B^2 L^2 \right) \\ b_t & = 2\beta p s \eta_t \left(\sqrt{\epsilon} (G + \sigma) + \frac{\kappa(s-1)\eta_t L}{2} (G + \sigma) \right), \\ c_t & = \beta^2 p s^2 \eta_t^2 \left(1 + \frac{\kappa(s-1)\eta_t L}{2} \right)^2 (G^2 + \sigma^2). \end{aligned}$$

Using the fact that $\Delta_t \leq \frac{a_t}{2b_t} \Delta_t^2 + \frac{b_t}{2a_t}$, and taking expectation over \mathcal{F}_t we get that

$$\mathbb{E}[\Delta_{t+1}^2] \leq \left(1 - \frac{a_t}{2} \right) \mathbb{E}[\Delta_t^2] + \frac{b_t^2}{2a_t} + c_t,$$

Unrolling the recursion, we deduce that

$$\mathbb{E}[\Delta_t^2] \leq \prod_{\tau=0}^{t-1} \left(1 - \frac{a_\tau}{2} \right) \Delta_0 + \sum_{\tau=0}^{t-1} \left(\frac{b_\tau^2}{2a_\tau} + c_\tau \right) \prod_{\tau'=\tau+1}^{t-1} \left(1 - \frac{a_{\tau'}}{2} \right).$$

Choose $\eta_t = \frac{\theta}{t+\gamma}$ for some constants θ and γ such that $\beta p s \mu \theta \geq 2$ and $\theta/\gamma \leq \mu/(20\beta s L^2 B^2)$. Then $\eta_t \leq \frac{\theta}{\gamma} \leq \frac{\mu}{20\beta s L^2 B^2}$. Therefore, $\eta_t \beta s L^2 B^2 \leq 0.1\mu$ and $\eta_t s L \leq 0.1$. Furthermore, $\kappa \leq \frac{e^{0.1}-1-0.1}{(0.1)^2/2}$. By the standing assumption, $\sqrt{\epsilon}B \leq 0.1\mu/L$ and hence $a_t \geq 2C_0\beta p s \eta_t \mu$. for some constant $C_0 \geq$

$1 - 0.1 - 0.05\kappa - 0.05(1 + 0.05\kappa)^2 \geq 0.7929$. Let $\rho = C_0\beta ps\theta\mu$. By our choice of θ , $\rho > 1.5$. Then it follows that

$$\prod_{\tau'=\tau}^{t-1} \left(1 - \frac{a_{\tau'}}{2}\right) \leq \exp\left(-\frac{1}{2} \sum_{\tau'=\tau}^{t-1} a_{\tau'}\right) \leq \exp\left(-\rho \sum_{\tau'=\tau}^{t-1} \frac{1}{\tau' + \gamma}\right) \leq \exp\left(-\rho \log\left(\frac{t + \gamma}{\tau + \gamma}\right)\right),$$

where the last inequality holds because $\sum_{\tau'=\tau}^{t-1} \frac{1}{\tau' + \gamma} \geq \int_{\tau+\gamma}^{t+\gamma} \frac{1}{x} dx = \log \frac{t+\gamma}{\tau+\gamma}$. Moreover, $a_t/2 \leq \beta ps\eta_t\mu \leq \frac{\mu^2 p}{20L^2 B^2} \leq 0.05$, so that $1 - a_t/2 \geq 0.95$. Hence,

$$\begin{aligned} \frac{1}{1 - a_t/2} \left(\frac{b_t^2}{2a_t} + c_t\right) &\leq \frac{\beta(2ps\eta_t)^2 2(\epsilon + (C_1 s L \eta_t)^2)}{0.95 \cdot 4C_0 \beta ps\eta_t\mu} (G + \sigma)^2 + C_2 \beta^2 ps^2 \eta_t^2 (G + \sigma)^2 \\ &\leq \frac{2}{0.95C_0} \epsilon (G + \sigma)^2 \beta ps\eta_t/\mu + C' \beta^2 ps^2 \eta_t^2 (G + \sigma)^2, \end{aligned}$$

where C_1, C_2, C' are some universal constants and the last inequality uses the fact that $\eta_t \beta s L^2 \leq 0.1\mu$. Therefore,

$$\left(\frac{b_\tau^2}{2a_\tau} + c_\tau\right) \prod_{\tau'=\tau+1}^{t-1} \left(1 - \frac{a_{\tau'}}{2}\right) \leq (G + \sigma)^2 \left(\frac{2\epsilon \beta ps\theta}{0.95C_0\mu(\tau + \gamma)} + \frac{C' \beta^2 ps^2 \theta^2}{(\tau + \gamma)^2}\right) \left(\frac{t + \gamma}{\tau + \gamma}\right)^{-\rho}.$$

It follows that

$$\begin{aligned} &\sum_{\tau=0}^{t-1} \left(\frac{b_\tau^2}{2a_\tau} + c_\tau\right) \prod_{\tau'=\tau+1}^{t-1} \left(1 - \frac{a_{\tau'}}{2}\right) \\ &\leq \frac{2}{0.95C_0} \epsilon (G + \sigma)^2 \beta ps\theta\mu^{-1} (t + \gamma)^{-\rho} \sum_{\tau=0}^{t-1} (\tau + \gamma)^{\rho-1} \\ &\quad + C' (G + \sigma)^2 \beta^2 ps^2 \theta^2 (t + \gamma)^{-\rho} \sum_{\tau=0}^{t-1} (\tau + \gamma)^{\rho-2} \\ &\leq \frac{2}{0.95C_0} \epsilon (G + \sigma)^2 \beta ps\theta/(\rho\mu) + C' (G + \sigma)^2 \frac{\beta^2 ps^2 \theta^2}{\rho - 1} \frac{1}{t + \gamma}. \end{aligned}$$

In conclusion, we get that

$$\mathbb{E} [\Delta_t^2] \leq (1 + t/\gamma)^{-\rho} \Delta_0 + \frac{2\epsilon}{0.95C_0^2\mu^2} (G + \sigma)^2 + C' (G + \sigma)^2 \frac{\rho^2}{(\rho - 1)p\mu^2} \frac{1}{t + \gamma},$$

where $2/(0.95C_0^2) \leq 2/(0.95 \times 0.7929^2) < 4$.

The proof for FedProx is completely analogous. The only difference is that we need to apply Lemma B.1 instead of Lemma 5.1 to bound the perturbation of the local proximal step. In the end, we get that

$$\mathbb{E} [\Delta_{t+1}^2 \mid \mathcal{F}_t] \leq (1 - a'_t) \Delta_t^2 + b'_t \Delta_t + c'_t,$$

where

$$\begin{aligned} a'_t &= 2\beta p\eta_t \left(\mu - \sqrt{\epsilon}BL - \frac{\eta_t L}{1 - \eta_t L_-} BL - \beta \frac{\eta_t}{2} \left(1 + \frac{\eta_t L}{1 - \eta_t L_-}\right)^2 B^2 L^2\right), \\ b'_t &= 2\beta p\eta_t \left(\sqrt{\epsilon}(G + \sigma) + \frac{\eta_t L}{1 - \eta_t L_-} (G + \sigma)\right), \\ c'_t &= \beta^2 p\eta_t^2 \left(1 + \frac{\eta_t L}{1 - \eta_t L_-}\right)^2 (G^2 + \sigma^2). \end{aligned}$$

Following the same steps as above, we can further deduce that

$$\mathbb{E} [\Delta_t^2] \leq (1 + t/\gamma)^{-\rho} \Delta_0 + \frac{2\epsilon}{0.95C_0^2\mu^2} (G + \sigma)^2 + C' (G + \sigma)^2 \frac{\rho^2}{(\rho - 1)p\mu^2} \frac{1}{t + \gamma},$$

where $\rho = C_0\beta p\theta\mu > 1.1$ and $C_0 \geq 0.727$ so that $2/(0.95C_0^2) < 4$. \square

C Experiments

In this section, we provide the detailed setups and additional experiments.

Hardware environments: we run all the experiments on a cluster with 8 Tesla V100 Volta GPUs and 80 Intel Xeon E5 CPUs. The codes are built upon PyTorch 1.13.1 [42].

Implementation details: For the numerical calculation of GM, we adopt the smoothed Weiszfeld algorithm from [37]. To adapt to clients with quantify skewness, the iterative centered clipping rule is modified to

$$\mathbf{v}_{l+1} = \mathbf{v}_l + \sum_{i=1}^M w_i (\theta_i - \mathbf{v}_l) \min \left(1, \frac{\tau_l}{\|\theta_i - \mathbf{v}_l\|_2} \right), \quad (44)$$

where the choice of $\tau_l = \frac{10}{1-\beta_0}$ follows from [27], and β_0 is the momentum coefficient. Likewise, Line 9 in Algorithm 1 of [7] is modified to

$$\theta_{t+1} = \theta_t - \eta_t \sum_{i=1}^M w_i G^i. \quad (45)$$

C.1 CIFAR-10

We present the additional experiments on CIFAR-10 dataset under light unavailability scheme with $\epsilon = 0.2$. The results are shown in Fig. 7 and 8. Generally, the observations resemble those from the case of $\epsilon = 0.8$. Our variants' trajectories are less fluctuating than the naive FedAvg and FedProx algorithms. In the baseline comparisons, all the FedAvg-type algorithms achieve

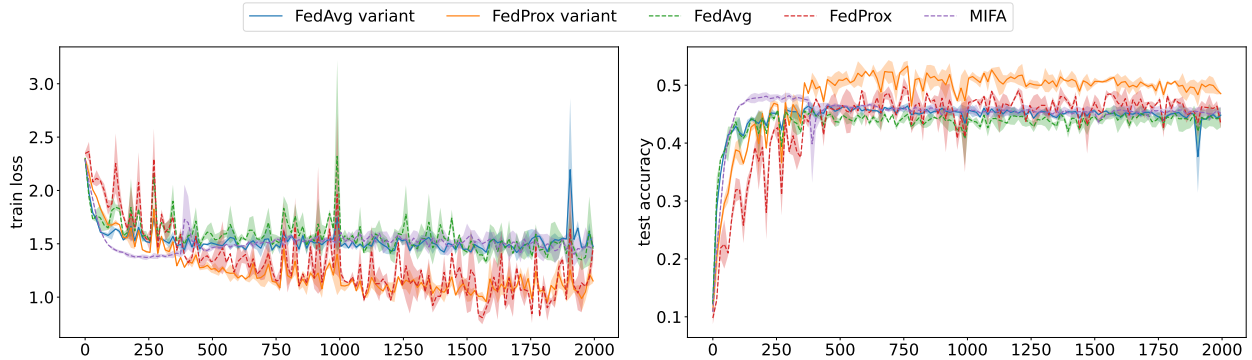


Figure 7: CIFAR-10 results with Dirichlet parameter $\alpha = 0.1$ and dropout fraction $\epsilon = 0.2$ baseline comparisons on adversarial client unavailability scheme in Section 7.1.

comparable performance, while our FedProx variant achieves the best test accuracy. The Byzantine-resilient algorithms, except the naive GM, reach similar results as well, as a total of eight clients participate in the training per round. This is in sharp contrast to the highly adversarial case of $\epsilon = 0.8$, where only two clients are responsive in each round.

C.1.1 Prolonged training from 2000 rounds to 4000 rounds of CIFAR-10.

Since the bucketing-GM, bucketing-cclip, GM, and cclip do not appear to have converged in Fig. 8, we further increase the training horizon from 2000 communication rounds to 4000 rounds in Fig. 11a. There are indeed improvements in training for bucketing-cclip and bucketing-GM with respect to train loss and test accuracy; however, the FedProx variant still achieves the best performance. The final average loss and accuracy of our variants are plotted as horizontal lines for a neat presentation. It is worth noting that the Byzantine algorithms we adopt in the numerical evaluations are not the original algorithms proposed by the authors since the original ones do not apply to our system setup.

C.2 Synthetic datasets

We present the additional experiments on the synthetic datasets with $\epsilon = 0.7$. The results are shown in Fig. 9 and 10. Again, the trends are similar to Section 7.4. In all the experiments, the proposed variants progress smoothly and achieve similar or better performances compared with other baselines. More importantly, the performance does not demand additional memory, unlike MIFA or the Byzantine-resilient algorithms.

C.2.1 Prolonged training from 2000 rounds to 4000 rounds for synthetic datasets.

We also increased the training horizon from 2000 communication rounds to 4000 rounds on Synthetic (1,1) data in Fig. 11b. All the algorithms achieve comparable test accuracy, while the algorithms of the same types (FedAvg-type and FedProx-type) reach alike train losses. We group the numerical results of the original algorithms (FedAvg and FedProx) and the proposed variants into two zoom-in boxes. The scrutiny reveals that the trajectories of the proposed variants are more smooth when compared with the original ones. This matches our anticipation. It is worth noting that Eq. (3) of our submission is equivalent to $\theta_{t+1} = (1 - \beta \sum_{i \in \mathcal{S}_t} w_i) \theta_t + \beta \sum_{i \in \mathcal{S}_t} w_i \theta_{i,t+1}$. By choosing β so that $\beta \sum_{i \in \mathcal{S}_t} w_i < 1$, we are smoothing the trajectory of θ_t .

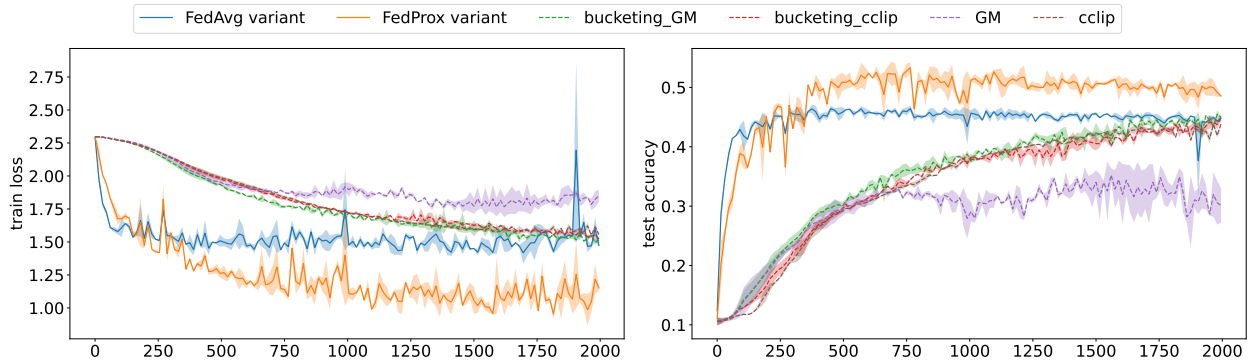


Figure 8: CIFAR-10 results with Dirichlet parameter $\alpha = 0.1$ and dropout fraction $\epsilon = 0.2$ Byzantine comparisons on adversarial client unavailability scheme in Section 7.1.

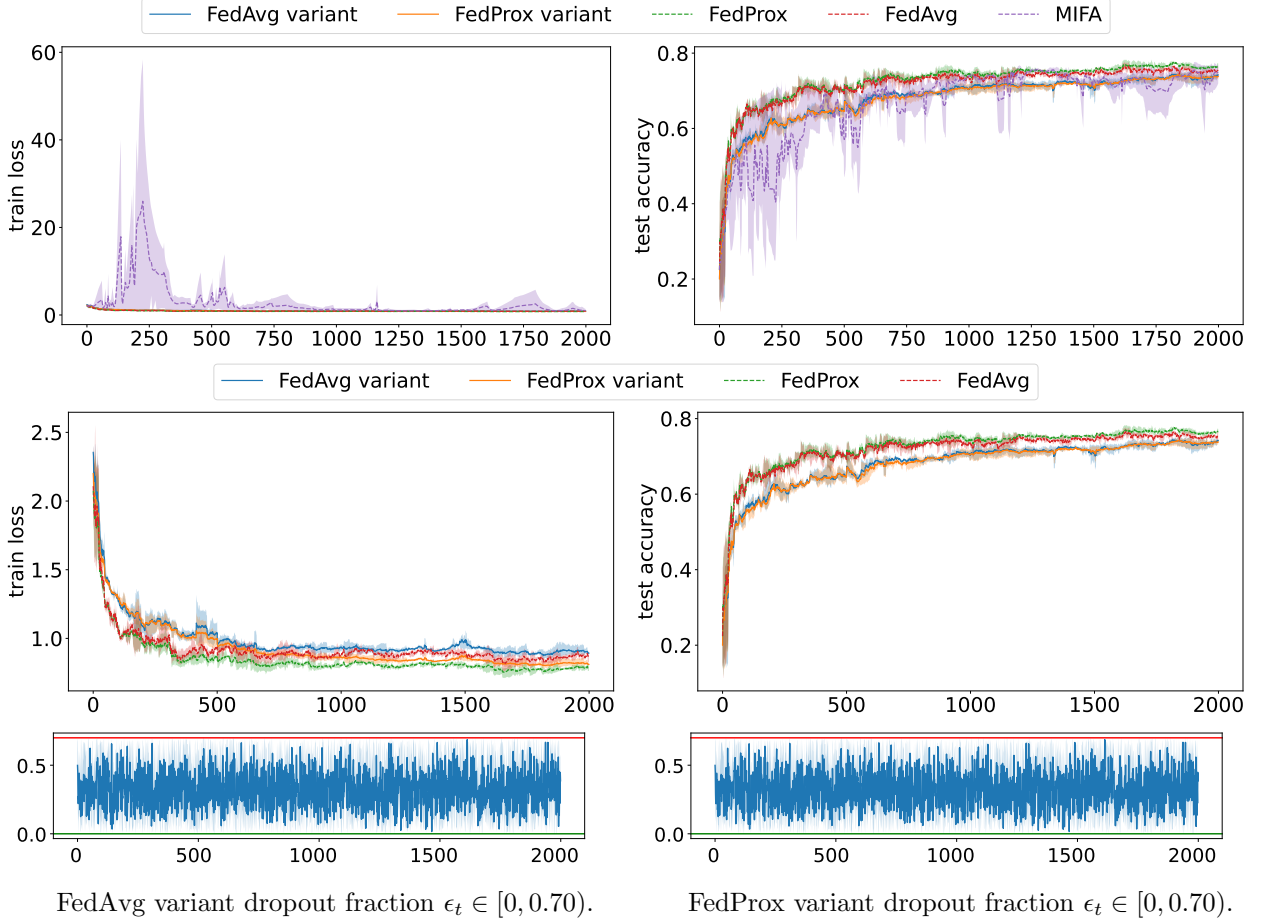


Figure 9: Synthetic datasets: baseline comparisons with dropout fraction $\epsilon = 0.7$ on adversarial client unavailability scheme in Section 7.1.

C.3 Additional attacks: Round-robin adversary and random responsive probability

We also test the variants of FedAvg and FedProx against another dropout scheme, which we refer to as *round-robin attack*. Our results can be found in Fig. 12 and Fig. 13. The adversary randomly partitions the clients into r equal-sized groups and assigns each group with a label in $\{0, \dots, r-1\}$. During t -th communication round for $100(i-1) < t \leq 100i$, all clients from the group with the label $i \pmod{r}$ will be unresponsive, i.e., the groups become unavailable in a round-robin fashion every 100 rounds. In every round, there are $(1/r)$ -fraction of unresponsive clients on average.

We considered the sort-and-partition scheme to generate non-IID datasets: A total of 100 clients each holding image samples of 2 classes from *CIFAR-10* dataset. This follows [31] and yields highly non-IID data. Specifically, as we have 10 data classes in *CIFAR-10* datasets, we partition the 100 clients into 5 groups with equal sizes. We assign each group an ID $\in [5]$. The clients in the group ID will be assigned the images from the classes $\{2\text{ID} - 1, 2\text{ID}\}$. In each communication round, a client draws a batch of 10 samples from the local dataset.

In each communication round, $|\tilde{\mathcal{S}}_t| = K \in \{5, 10, 30\}$ clients are randomly sampled. Clients will be dropped by the adversary according to the schemes we discussed. In all figures, the plots from top to bottom are with $K = 5, 10, 30$, respectively. The plots from left to right are of $r = 4, 5, 10$,

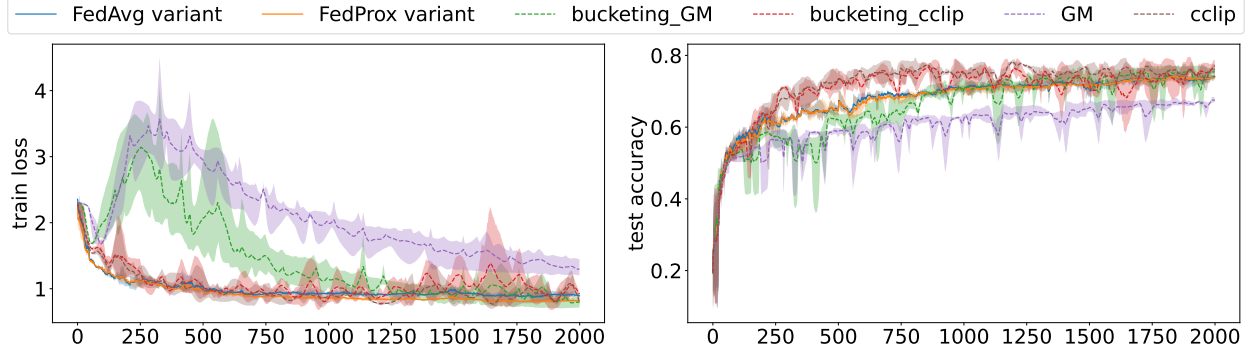
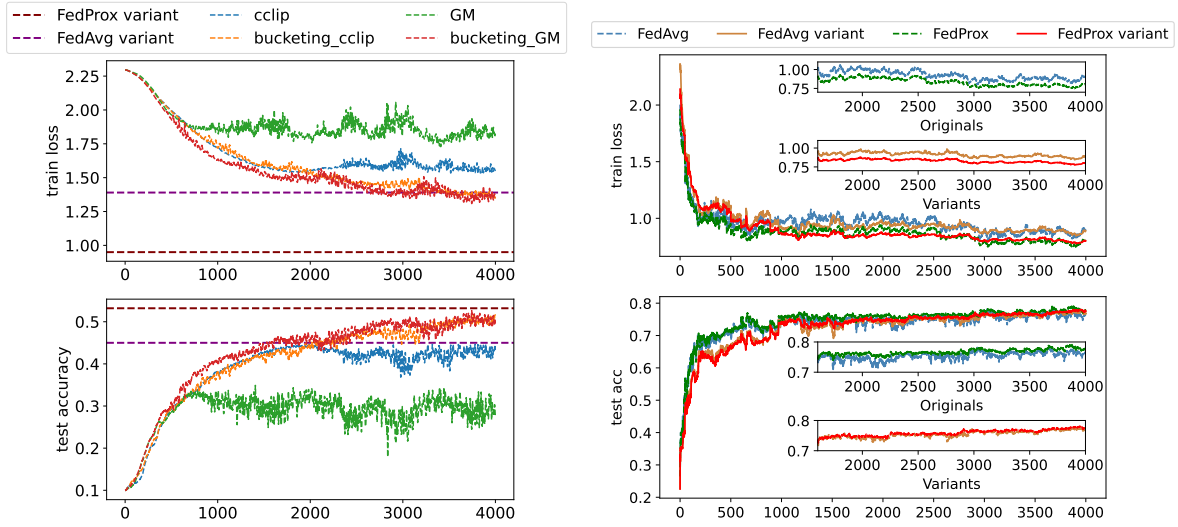


Figure 10: Synthetic datasets: Byzantine comparisons with dropout fraction $\epsilon = 0.7$ on adversarial client unavailability scheme in Section 7.1.



(a) The results of Fig. 8 after prolonged training. (b) The results of Fig. 8 after prolonged training.

Figure 11: The plots of Fig. 8 after extending the training time from 2000 rounds to 4000 rounds.

respectively.

It is observed from Fig. 4 that the FedAvg variant with $\beta = \sqrt{M/K}$ beats all the other algorithms. The increase in K helps to smooth out the curves. Empirically, the increase in β from 1 to $\sqrt{M/K}$ introduces acceleration in training.

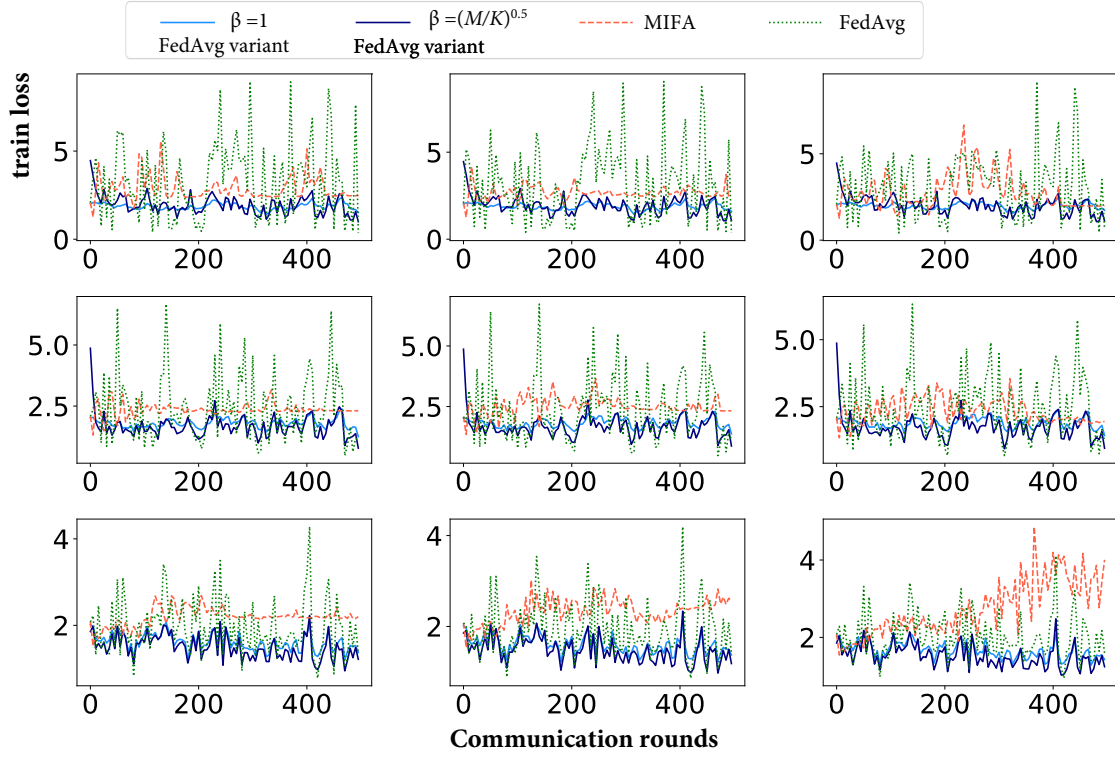


Figure 12: Train loss of round-robin adversaries on *CIFAR-10* dataset.

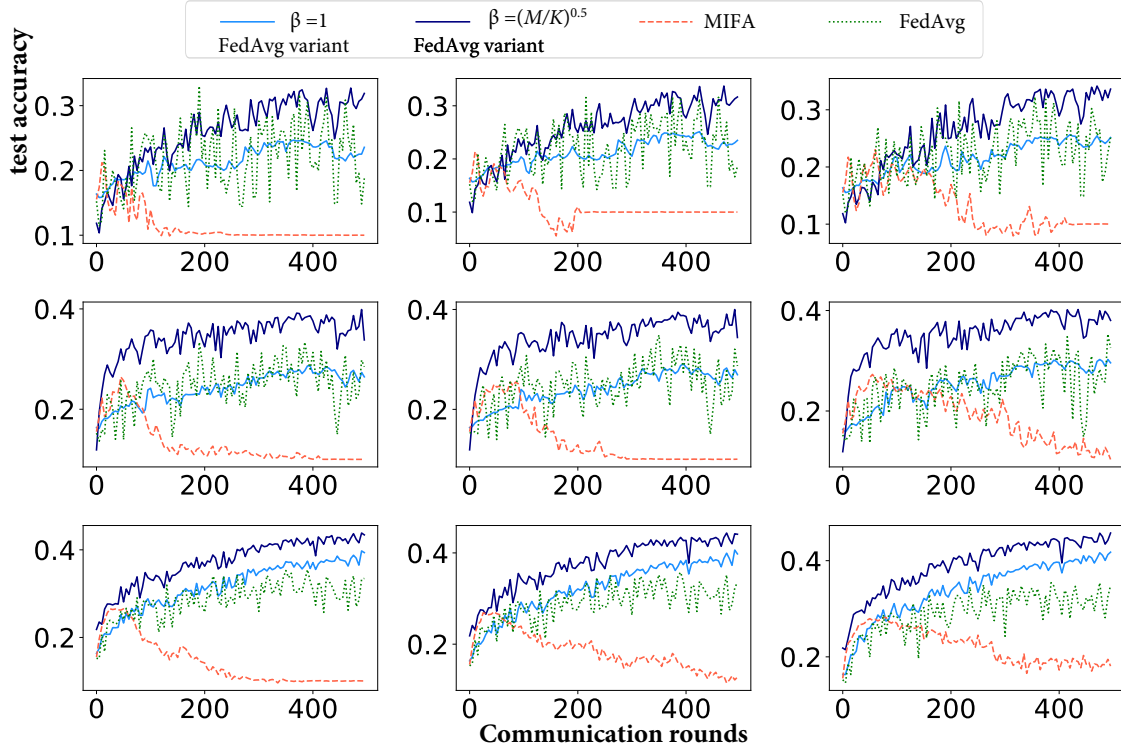


Figure 13: Test accuracy on *CIFAR-10* dataset.